

Microscopic theory of displacive ferroelectricity: applications to quantum criticality and classical phase transitions

F. Yang^{1,*} and L. Q. Chen^{1,†}

¹*Department of Materials Science and Engineering and Materials Research Institute,
The Pennsylvania State University, University Park, PA 16802, USA*

(Dated: December 19, 2024)

Accurate quantitative prediction of the finite-temperature properties of a phase transitioning system has been a long-standing challenge in condensed matter physics and materials science. Here we regard a collective vector mode as essential quasiparticle excitation of the displacive ferroelectricity. Starting from the quantum statistic description of this excitation, we develop a self-consistent, microscopically based phase-transition theory of displacive ferroelectricity. This theory enables one to use only the ground-state properties to predict the finite-temperature properties and in particular, the criticality of phase transitions, in a striking contrast to the widely used Landau-Ginzburg phenomenological description near the critical point. Its applications to the quantum paraelectrics SrTiO₃ and KTaO₃ as well as the classical ferroelectric PbTiO₃ demonstrate remarkable quantitative agreements with the experimentally measured critical behaviors of the phase transitions and the corresponding dielectric/ferroelectric properties throughout the entire temperature ranges of the phases without fitting parameters. The theory should be general and can be utilized to understand a broad range of phase transitions in other bosonic systems.

Introduction.—In the quantum statistic theory of condensed matter systems [1], quasiparticle excitations emerge in an ordered quantum phase associated with a spontaneous breaking of the continuous symmetry after the condensation [2]. These excitations determine the macroscopic characteristics of the system, including the critical behaviors of the phase, and has lead to a far-reaching relevance of physics. For example, due to a similar mechanism, the collective amplitude mode of the order parameter in an ordered phase [3] resembles the Higgs particle in particle physics [4, 5], which gives mass to elementary particles in the standard model, and this mode so far has been identified in a variety of the contexts, extending to conventional [6–9] and unconventional [10, 11] superconductors, superfluids [12, 13], a subclass of antiferromagnets [14–16], charge density waves [17–19] and ferroelectrics [20].

The quasiparticle description allows one to predict the finite temperature properties of the system and the critical behaviors of the phase based on only the knowledge about the ground state at zero temperature. This fundamental description has been successfully applied to ferromagnetic/antiferromagnetic systems and conventional superconductors [21]. There have also been a few attempts for the displacive ferroelectricity [22–27], starting from the ground state, but the resulted predictions by including appropriate fluctuation corrections have been largely qualitative in the specific ferroelectric materials [28].

The majority of the current theoretical and computational efforts in understanding the thermodynamics of the ferroelectrics have employed the Monte-Carlo simulations based on first-principles effective Hamiltonian [29–36], self-consistent lattice dynamics [37–40] and empirical/machine-learned potentials [41–43], or phenomenological models within Landau-Ginzburg theory [27, 44–47]. While the computational first-principles calculations have been extremely useful for understanding relative structural stability of different ground states

of a ferroelectric crystal, they often failed to provide accurate/consistent predictions of the properties in the entire temperature range of the phase and critical behaviors, particularly the transition temperatures [40, 42]. On the other hand, phenomenological models assume the knowledge of known critical behaviors (e.g., critical temperature) and often have poor descriptions of the ferroelectric properties towards low temperatures far away from the critical point.

Here motivated by the quantum criticality theory [22, 24, 25] and experimental progress [22], we propose a self-consistent thermodynamic theory of displacive ferroelectricity based on the quantum statistic theory of quasiparticle excitations. The collective amplitude mode in displacive ferroelectrics is the amplitude fluctuation of the long-range ordered polarization, or called “ferron” [20]. Extending this concept, we regard the essential excitation as a collective vector mode, i.e., the vector fluctuation of the long-range ordered polarization. By deriving the excitation of this mode, consisting of the zero-point oscillation and thermal excitation, we develop a self-consistent renormalization from the ground-state Lagrangian to finite-temperature free energy of the long-range ordered polarization. This offers a microscopic phase-transition theory of the displacive ferroelectricity, and enables one to use only the ground-state parameters to predict the dielectric/ferroelectric properties at finite temperatures in the entire range of the phase and in particular, criticality of the phase, in contrast to the widely used Landau-Ginzburg theories around critical point. For the first time, we are able to quantitatively predict the dielectric/ferroelectric properties and criticalities for two types of representative materials systems, the quantum paraelectrics SrTiO₃ and KTaO₃ on the verge of ferroelectricity and the classical ferroelectric PbTiO₃, in excellent quantitative agreement with existing experimental measurements in the entire temperature range of the phase without fitting parameters.

Results.—The displacive ferroelectricity is widely suggested to originate from an unstable optical phonon mode [48–54], which has imaginary frequencies (i.e., negative values of the harmonic terms in lattice dynamics) at the zone center.

* fzy5099@psu.edu

† lqc3@psu.edu

The imaginary-frequency phonons undergo a condensation at certain temperature, whereas the remaining gapless real-frequency phonons on this phonon branch acquire an excitation gap after the condensation and evolve into the experimentally observed optical soft phonon mode. In the mean field theory, one can single out the imaginary-frequency phonons and describe the lattice distortion by an order-parameter field [55]:

$$\xi = \langle |b_{\text{sp}}^\dagger| \rangle, \quad (1)$$

resulting in a polarization field $\mathbf{P} = (z^* \mathbf{u} / \Omega_{\text{cell}}) \xi$ [48–54]. Here, b_{sp}^\dagger is the creation operator of the imaginary-frequency phonons; \mathbf{u} represents the distortion vector; z^* and Ω_{cell} stand for the effective charge and unit-cell volume, respectively. Due to the condensation and lattice dynamics [48–54], the ground state of the order-parameter field ξ is captured by the quantum-field- ϕ^6 model [56], leading to the Lagrangian of the polarization field for the displacive ferroelectricity [22–25, 27, 57]:

$$\mathcal{L} = \frac{m_p}{2} (\partial_t P)^2 - \left[\frac{g}{2} (\nabla P)^2 + \frac{a}{2} P^2 + \frac{b}{4} P^4 + \frac{\lambda}{6} P^6 \right], \quad (2)$$

where a , b , λ are model parameters; g is related to the velocity of the imaginary-frequency phonons [22] and m_p is the polarization inertia [20]. We emphasize that the polynomial expression here is a result of the lattice dynamics rather than Landau expansion of the order parameter near critical point.

The polarization field $\mathbf{P} = \mathbf{P}_r + \delta\mathbf{P}$, consisting of the long-range ordered polarization \mathbf{P}_r and polarization fluctuation $\delta\mathbf{P}$. In renormalization theory, with a vanishing thermally averaged $\langle \delta\mathbf{P} \rangle$ but a nonzero thermally averaged $\langle \delta P^2(T) \rangle$, one can extract the contributions purely from the long-range ordering:

$$F = \int d\mathbf{x} \left[\frac{\alpha(T)}{2} P_r^2 + \frac{\beta(T)}{4} P_r^4 + \frac{\lambda}{6} P_r^6 \right], \quad (3)$$

where

$$\alpha = a + b(2/d_p + 1) \langle \delta P^2(T) \rangle + \lambda(4/d_p + 1) (\langle \delta P^2(T) \rangle)^2, \quad (4)$$

$$\beta = b + 2\lambda(4/d_p + 1) \langle \delta P^2(T) \rangle, \quad (5)$$

with d_p being the dimension of the vector space of $\delta\mathbf{P}$.

The fluctuation part $\langle \delta P^2(T) \rangle$ can be derived within the quantum statistic mechanism [1] and is related to the microscopic bosonic excitation of a collective mode that emerges after the condensation of the imaginary-frequency phonons (see Methods). This quasiparticle excitation has an energy spectrum $\hbar\omega_{\text{vm}}(q, a, b, P_r^2, \langle \delta P^2 \rangle) = \hbar\sqrt{\Delta^2(a, b, P_r^2, \langle \delta P^2 \rangle) + gq^2/m_p}$ with q being the wave vector, and its excitation gap is given by

$$\Delta(a, b, P_r^2, \langle \delta P^2 \rangle) = \left[a + b(2/d_p + 1)P_r^2 + \lambda(4/d_p + 1)P_r^4 + b\langle \delta P^2 \rangle + \lambda\langle \delta P^2 \rangle^2 + 2\lambda(4/d_p + 1)P_r^2\langle \delta P^2 \rangle \right]^{1/2} / \sqrt{m_p} \quad (6)$$

which requires a self-consistent calculation due to dependence on $\langle \delta P^2 \rangle$ and P_r^2 . The collective mode here is in fact a vector mode as it describes the vector fluctuation of the long-range ordered polarization. The obtained F describes the finite-temperature free energy of the long-range ordered polarization, and its minimum gives rise to $P_r^2 \neq 0$ for $\alpha < 0$ representing

the ferroelectric phase and $P_r^2 = 0$ for $\alpha > 0$ representing the paraelectric phase. The original parameters a and b for determining P_r^2 in the ground state are then renormalized to $\alpha(T)$ and $\beta(T)$ for finite temperatures. Fundamentally, this renormalization is equivalent to the derivation of the effective action (i.e., partition function) of the long-range ordered polarization \mathbf{P}_r within the path-integral approach, by self-consistently integrating out the fluctuation $\delta\mathbf{P}$ in Matsubara representation from the initial action. The self-consistent treatment here can avoid the infinite-order self-energy corrections by fluctuations.

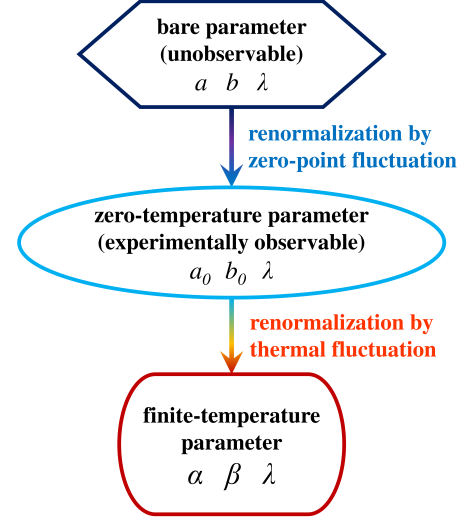


FIG. 1. Schematic of the renormalization in thermodynamic theory.

Due to the bosonic excitation of the vector mode, $\langle \delta P^2(T) \rangle$ consists of the thermal fluctuations $\langle \delta P_{\text{th}}^2(T) \rangle$ and zero-point fluctuations $\langle \delta P_{\text{zo}}^2 \rangle$. The thermal fluctuations are zero at $T = 0$ and become finite at $T \neq 0$. The zero-point fluctuations are quantum fluctuations and are nonzero at $T = 0$. In the quantum field theory, the zero-point fluctuations are integrated to the vacuum state [56], and hence, the vacuum state is not truly empty as the original/bare one but instead contains various excitations that pop into and out of the vacuum. The zero-point fluctuations of the polarization in displacive ferroelectrics has long been overlooked or not been seriously taken account of in existing theories [22–27]. As shown in Fig. 1, here we consider that the ground-state parameters a and b , which can in principle be obtained from the first-principles calculations, are experimentally unobservable. Only through the renormalization by zero-point fluctuations, a and b become the zero-temperature parameters a_0 and b_0 that can be experimentally measured. Further applying the renormalization by thermal fluctuations leads to the free-energy parameters $\alpha(T)$ and $\beta(T)$ at finite temperatures. The details of this renormalization within a self-consistent formulation are provided in Methods.

It should be emphasized that for accuracy, one can directly start with the experimentally measured zero-temperature parameters if they are available and perform the renormalization by thermal fluctuations to obtain the finite-temperature dielectric properties. However, if only the bare parameters are available from the first-principles calculations, the renormal-

ization by zero-point fluctuations is required and critical for the accurate predictions of the dielectric properties and criticality.

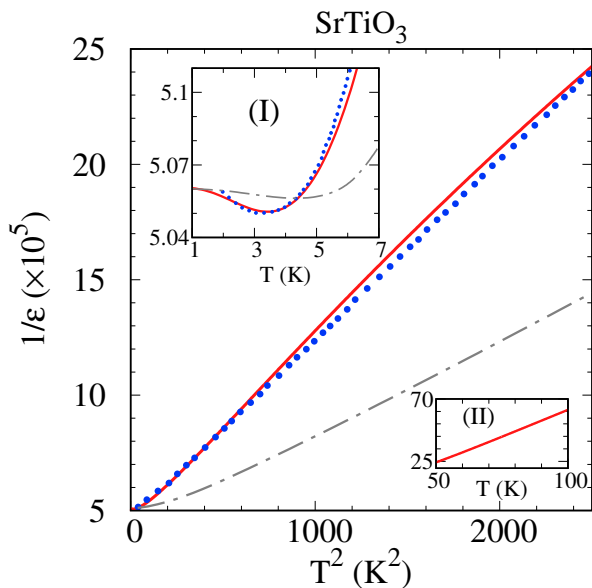


FIG. 2. Temperature dependence of the inverse dielectric function in quantum paraelectric SrTiO₃. The main figure is plotted versus the square of the temperature up to 50 K to compare with the experimental data. The red solid curve are predicted values from the present theory. The specific zero-temperature parameters, and their determination using several independent measurements are addressed in Supplementary Materials. The blue dots and gray chain curve come from the experimental measurement and quantum criticality theory in Ref. [22], respectively. The insets (I) and (II) show the results versus T at low and high temperatures.

To demonstrate the applications of the proposed theory, we first consider the textbook examples of displacive quantum paraelectrics SrTiO₃ and KTaO₃ [22, 51, 58, 59], which provide a promising candidate to examine the theory on the paraelectric side of displacive ferroelectricity. The structures of SrTiO₃ and KTaO₃ are found to be cubic perovskite ($d_p = 3$) at room temperature. While KTaO₃ remains as cubic down to low-temperature limit [60], SrTiO₃ undergoes a cubic-to-tetragonal antiferrodistortive transition at 105 K [51, 61, 62], but its tetragonality of 1.00056 is very small, causing essentially no change in the cell volume, thermal-expansion coefficient, or dielectric properties at the antiferrodistortive transition [63, 64]. Existing experimental measurements also show $\lambda \approx 0$ in SrTiO₃ and KTaO₃. Therefore, according to our theory, $\beta(T) = b_0 = b$ can be considered as temperature-independent and not affected by renormalization, so we only need to focus on the renormalization of a to $\alpha(T)$.

In the so called quantum paraelectrics, there exists a strong competition between the quantum fluctuation and ferroelectric ordering [65], i.e., there exist the unstable phonon modes related to the ferroelectricity, but the zero-point vibrations of the lattice dynamics prevent the dipole correlation from the long-range ordering [58, 59]. Our calculation of the self-consistent renormalization (see Supplementary Materials) also finds that because of the existence of the unstable phonon mode [40],

SrTiO₃ with a bare parameter $a < 0$ by first-principles calculations [40] should undergo a transition to ferroelectric phase at a low temperature, but the zero-point oscillation of the collective vector mode prevents the formation of the long-range ferroelectric ordering, leading to an incipient ferroelectricity with a nearly vanishing $a_0 > 0$. This theoretical/analytical description confirms the established understanding of the quantum paraelectric ground state of SrTiO₃ in the literature. Because of this character, we assume that the collective vector mode in this case can persist to exist and is uninterrupted in a wide temperature range above zero. As a result, its thermal excitation is expected to prohibit the ferroelectric ordering.

Through the renormalization by thermal fluctuations on the experimentally measured $a_0 > 0$ [22], we predict the dielectric properties of quantum paraelectrics SrTiO₃ and KTaO₃ at finite temperatures, and plot their inverse dielectric functions in Figs. 2 and 3. As seen from the figures, the predicted temperature dependencies of $1/\varepsilon(T)$ from the present theory almost completely quantitatively coincide with the experimental measurements. It should be emphasized that we achieve this remarkable quantitative agreement only using the zero-temperature parameters, determined from independent experimental measurements at low-temperature limit without fitting.

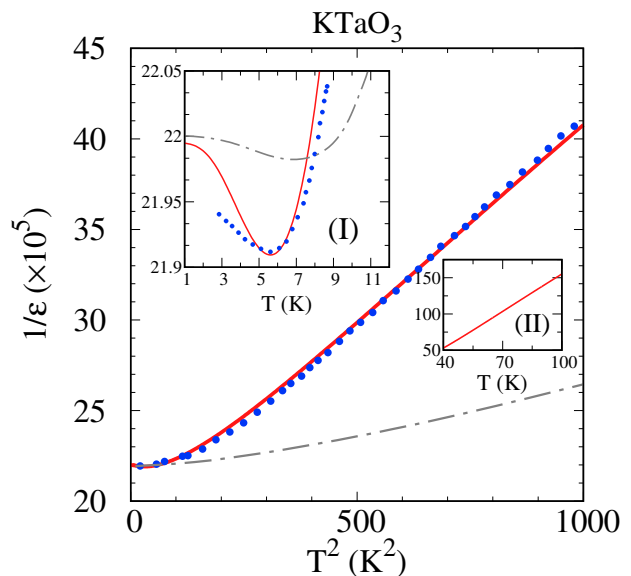


FIG. 3. Temperature dependence of the inverse dielectric function in quantum paraelectric KTaO₃. The main figure is plotted versus the square of the temperature up to 32 K to compare with the experimental data. The red solid curve are predicted values from the present theory. The specific zero-temperature parameters, and their determination using several independent measurements are addressed in Supplementary Materials. The blue dots and gray chain curve come from the experimental measurement and quantum criticality theory in Ref. [22], respectively. The insets (I) and (II) show the results versus T at low and high temperatures.

To gain insight into this quantum criticality, we examine the temperature dependence of dielectric functions closely. By $1/\varepsilon(T) \propto \alpha(T)$ and Eq. (4), one has $1/\varepsilon(T) \propto b_0 \langle \delta P_{\text{th}}^2(T) \rangle$. For the quantum paraelectrics with nearly vanishing a_0 and

$P_r^2(T) \equiv 0$, the excitation gap of the collective vector mode Δ [Eq. (6)] nearly vanishes near $T = 0$ and gradually increases with temperature due to the increased thermal fluctuation. This gap behavior in the bosonic thermal excitation leads to the T -square and linear- T dependencies of $\langle \delta P_{\text{th}}^2(T) \rangle$ at low and high temperatures (see Supplementary Materials), respectively. As

a result, the inverse dielectric function exhibits a non-classical T -square dependence in a wide temperature range, e.g., 5–50 K for SrTiO₃ (Fig. 2) and of 7–35 K for KTaO₃ (Fig. 3). Above this range, $1/\varepsilon(T)$ exhibits a classical linear- T (i.e., conventional Curie–Weiss) behavior, as shown in the insets (II) of Fig. 2 for SrTiO₃ and of Fig. 3 for KTaO₃.

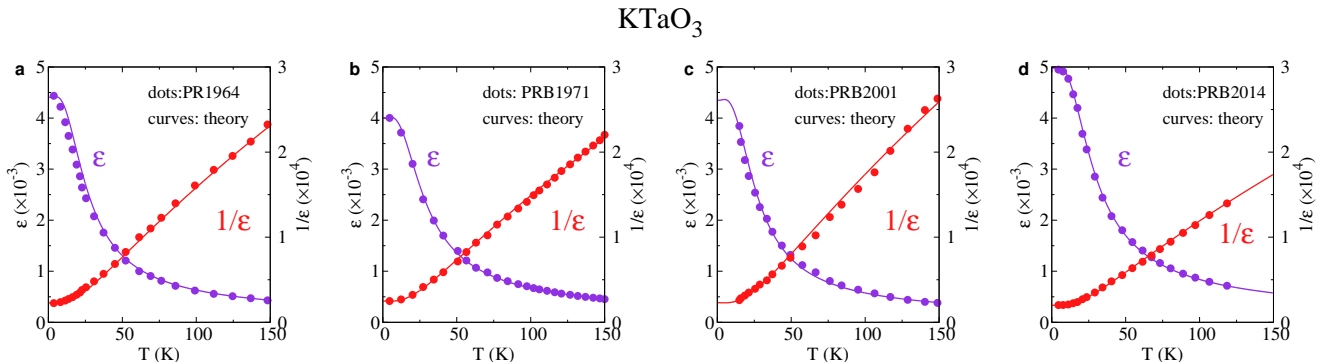


FIG. 4. Dielectric function and inverse dielectric function versus temperature in quantum paraelectric KTaO₃. In the figure, the dots come from the experimental measurements, and the solid curve are predicted values from the present theory. Experimental results in **a**, **b**, **c** and **d** come from Refs. [66], [67], [68] and [69]. The specific zero-temperature parameters, and their determination using experimental data at low-temperature limit are addressed in Supplementary Materials.

The measurement in Ref. [22] did not extend to the linear- T regime, while the linear- T behavior of $1/\varepsilon(T)$ at high temperatures has been reported in the literature in both SrTiO₃ [70] and KTaO₃ [66–69]. To validate our theory, we utilize several experimental reports [66–69] in KTaO₃ for comparison, and plot the dielectric functions in Fig. 4. For each experiment in the figure, the predicted temperature dependencies of the dielectric properties from our theory quantitatively coincide with the measured ones not only in the non-classical T -square regime at the relatively low temperatures but also in the classical linear- T regime at high temperatures.

At low-temperature limit, due to the minimal thermal fluctuation, the inverse dielectric function is expected to be insensitive to temperature variation and saturates to a plateau. However, with the decrease in temperature towards zero, experiments have observed a small upturn of $1/\varepsilon(T)$ below a few kelvin [22]. This anomalous upturn is suggested to be relevant to the coupling of the polarization field with gapless acoustic phonons through electrostrictive effect [22, 25, 28, 71]. Here we include this effect in the renormalization by adding a correction term related to thermal excitation of the acoustic phonons (see Methods and Supplementary Materials). The electrostrictive coefficient and parameters of the acoustic phonons used in our calculation are determined by independent measurements. The predicted results shown in the insets (I) of Fig. 2 for SrTiO₃ and of Fig. 3 for KTaO₃ also exhibit a quantitative agreement with the experimental measurements.

We next consider the ferroelectric side of the displacive fer-

roelectricity for a ferroelectric phase transition. The thermal excitation of the collective vector mode is expected to reduce the ferroelectric polarization with an increase in temperature from zero, thereby leading to the phase transition at certain critical temperature. To demonstrate the application of the proposed theory to classical ferroelectrics with high transition temperatures, we consider the ferroelectric PbTiO₃. As its crystal structure is tetragonal with a large distortion ratio 1.062 [27, 72], we re-write the Lagrangian as the one limited by the crystal symmetry (see Supplementary Materials) and derive the free energy of the long-range ordered polarization [Eq. (3)] through a self-consistent renormalization in Fig. 1.

The ferroelectric properties of PbTiO₃ predicted from the present theory are plotted in Fig. 5. As shown in Fig. 5a for the dielectric function $\varepsilon(T)$ or in Fig. 5b for the inverse dielectric function $1/\varepsilon(T)$, their temperature dependencies agree quantitatively with the experimentally measured values. Moreover, the dielectric properties below 100 K are insensitive to temperature due to the minimal thermal fluctuation. In the range of 200–600 K, $1/\varepsilon(T)$ (Fig. 5b) and $\alpha(T)$ (Fig. 5d) exhibit the classical linear- T dependencies as widely reported in the literature [45, 46, 73–75]. This behavior arises from $\langle \delta P_{\text{th}}^2 \rangle \propto T$ at 200–600 K (inset of Fig. 5d) due to the large energy gap Δ of the vector mode (see Supplementary Materials). Particularly, the obtained $\beta = 0.08175b_0 = -0.2943 \times 10^9 \text{ Jm}^5/\text{C}^4$ at 300 K from the developed theory (Fig. 5d) is very close to the experimentally measured room-temperature value of $\beta = -0.29 \times 10^9 \text{ Jm}^5/\text{C}^4$ which has been widely used in the

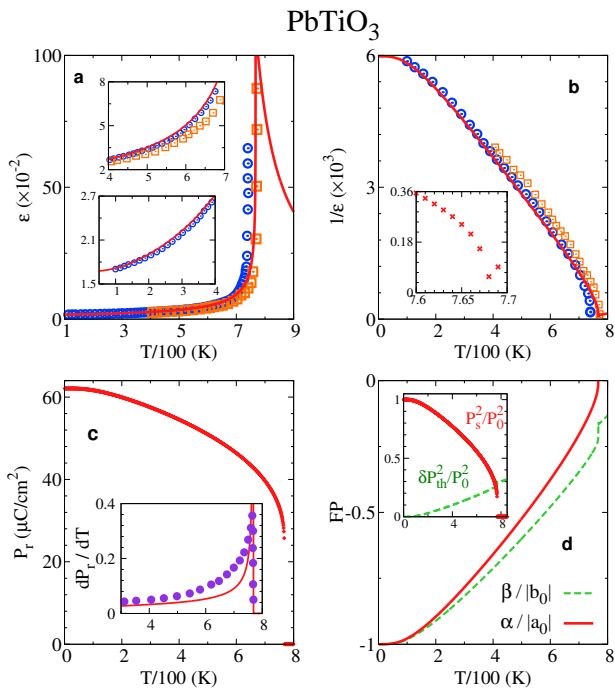


FIG. 5. Temperature dependence of the dielectric properties in ferroelectric PbTiO_3 . **a**, dielectric function; **b**, inverse dielectric function; **c**, spontaneous polarization; **d**, free-energy parameters α and β . Curves/crosses represent predicted values from the present theory. Orange squares (blue circles) in **a** and **b** are the experimental data from Ref. [73] (Ref. [74]). Insets of **a** and **b** zoom the corresponding temperature ranges. Inset of **c** shows the results of dP_r/dT , and the purple dots are the experimental data from Ref. [73]. Inset in **d** shows the fluctuation $\langle \delta P_{\text{th}}^2(T) \rangle$ and order parameter P_r^2 . The specific model parameters, and their determination using several independent measurements of the spontaneous polarization and dielectric function at long-temperature limit are discussed in Supplementary Materials.

literature [20, 45–47]. Above 600 K, the increased $\langle \delta P_{\text{th}}^2 \rangle$ approaches the reduced P_r^2 , causing a nearly vanishing gap Δ with rapidly enhanced fluctuation $\langle \delta P_{\text{th}}^2 \rangle$ and hence $\alpha(T)$ toward zero. In other words, the phase transition occurs around the point where the magnitude of order parameter fluctuation exceeds the magnitude of the order parameter.

The predicted transition temperature $T_c = 768$ K (the inset of Fig. 5b), in excellent agreement with existing experimentally measured value of 763 K [27, 72]. Moreover, according to the predicted temperature dependence of the long-range ordered polarization in Fig. 5c, the ferroelectric-paraelectric transition in PbTiO_3 is first-order, consistent with the widely reported experimental observation [27, 72]. The rate of variation of ferroelectric polarization with temperature or pyroelectric effect, dP_r/dT , also agrees with existing experimental measurements, as shown in the inset of Fig. 5c. To analyze this classical criticality of the ferroelectric phase transition, we plot $\alpha(T)$ and $\beta(T)$ as a function of temperature in Fig. 5d, and starting from $a_0 < 0$ and $b_0 < 0$ at $T = 0$, the correspondingly renormalized $\alpha(T)$ and $\beta(T)$ increase with temperature. The phase transition occurs at the temperature where $\alpha(T) = 0$, whereas $\beta(T)$ remains negative at this critical temperature (Fig. 5d),

and hence, the phase transition is first-order.

It should be emphasized again that the remarkable quantitative agreements between our theory predictions and the available experimental data in the ferroelectric PbTiO_3 are achieved with only the zero-temperature parameters from existing independent measurements at low-temperature and without fitting parameters. Therefore, the self-consistent microscopic phase-transition theory of the displacive ferroelectricity enables one to use only the ground-state parameters of a ferroelectric phase to predict the dielectric/ferroelectric properties at finite temperatures in the entire range of the ferroelectric phase including the classical criticality of the ferroelectric phase transition.

Discussion and summary.— We develop a self-consistent thermodynamic theory of the displacive ferroelectricity based on the quantum statistic theory of collective vector modes. Using this theory, without adjusting model parameters, we predict the finite-temperature thermodynamic and ferroelectric properties of quantum paraelectrics SrTiO_3 and KTaO_3 as well as classical ferroelectric PbTiO_3 , including their phase transition behaviors, in outstanding quantitative agreements with experimental measurements across the entire temperature range of the phases. This microscopic phase-transition theory offers a powerful theoretical tool enabling one to use only the ground-state parameters to predict the dielectric/ferroelectric properties at finite temperatures in the entire range of the phase and in particular, the phase transition criticalities.

The theory here is concerned with the long-range fluctuation, which should dominate the fluctuations over a large temperature regime above zero as the short-range/local excitation usually has a higher excitation energy. Compared with the previous theories of the displacive ferroelectricity [22–27], a unique treatment of the developed theory is the self-consistent formulation of the fluctuations and order parameter, which avoids calculating infinite-order self-energy corrections by fluctuations or picking up appropriate diagrammatic representations. Another ingredient is the incorporation of the zero-point fluctuation in Fig. 1, which follows the quantum-field theory for the vacuum state [56]. This treatment of the zero-point fluctuation should also be nontrivial and relevant to other subfields in condensed matter physics, as proved in recent theory of the disordered 2D superconductors for the zero-point superconducting phase fluctuation [76]. As seen from Figs. 2 and 3, without sufficiently self-consistent formulation of the excitation gap and without serious treatment of the zero-point fluctuation, the quantum criticality theory [22, 25], focusing on the border of an ordered phase, can provide the qualitative description, but is inadequate to provide quantitative one for the experimental measurements at finite temperatures.

The theory reported in this article should offer a useful theoretical tool for understanding and predicting many of the thermodynamic and nonequilibrium behaviors of displacive ferroelectricity, e.g., recently reported terahertz-induced ferroelectricity in quantum paraelectrics [58, 59] involving a nonequilibrium renormalization during optical excitation. Moreover, from a more fundamental viewpoint, this theory is a phase-transition theory of the Bose–Einstein condensation, and it may be relevant to understanding a broad range of the phase transitions in other bosonic systems, such as superfluids.

Acknowledgments

This work is supported by the US Department of Energy, Office of Science, Basic Energy Sciences, under Award Number

DE-SC0020145 as part of Computational Materials Sciences Program.

I. Method

We start with the Lagrangian of the polarization field in Eq. (2), which can be re-written as

$$\mathcal{L} = \frac{m_p}{2} (\partial_t \delta P)^2 - \left[\frac{g}{2} (\nabla \delta P)^2 + \frac{a}{2} \delta P^2 + \frac{b}{4} \delta P^4 + \frac{\lambda}{6} \delta P^6 \right] - \left[\frac{a}{2} P_r^2 + \frac{b}{4} P_r^4 + \frac{\lambda}{6} P_r^6 \right] - \left[\frac{b}{2} \left(\frac{2}{d_p} + 1 \right) P_r^2 \delta P^2 + \frac{\lambda}{2} \left(\frac{4}{d_p} + 1 \right) (P_r^4 \delta P^2 + P_r^2 \delta P^4) \right], \quad (7)$$

where we have taken the angular average of the fluctuations by neglecting their odd orders and considering isotropic fluctuations. Then, the thermally averaged contributions purely from the long-range ordering in Eq. (7) give rise to the free energy in Eq. (3). In addition, with this Lagrangian, the Euler-Lagrange equation of motion with respect to the polarization fluctuation $\delta \mathbf{P}$ leads to

$$\left[m_p \partial_t^2 + \gamma \partial_t - g \nabla^2 + a + b(2/d_p + 1) P_r^2 + \lambda(4/d_p + 1) P_r^4 + b \delta P^2 + \lambda \delta P^4 + 2\lambda(4/d_p + 1) P_r^2 \delta P^2 \right] \delta \mathbf{P} = \mathbf{E}_{\text{th}}(t, \mathbf{R}). \quad (8)$$

Here, we have introduced a damping rate $\gamma = 0^+$ and a thermal field $\mathbf{E}_{\text{th}}(t, \mathbf{R})$ that obeys the fluctuation-dissipation theorem [77]:

$$\langle \mathbf{E}_{\text{th}}(\omega, \mathbf{q}) \mathbf{E}_{\text{th}}(\omega', \mathbf{q}') \rangle = \frac{\gamma \hbar \omega (2\pi)^4 \delta(\mathbf{q} - \mathbf{q}') \delta(\omega - \omega')}{\tanh[\hbar \omega / (2k_B T)]}, \quad (9)$$

with the four-momentum $p = (\omega, \mathbf{q})$ being the Fourier space of the space-time coordinate $x = (t, \mathbf{R})$. Then, under the mean-field approximation, one can directly solve the thermally averaged polarization fluctuation:

$$\langle \delta P^2 \rangle = \int \frac{\hbar}{2m_p} \frac{\coth[\hbar \omega_{vm}(q, a, b, P_r^2, \langle \delta P^2 \rangle) / (2k_B T)]}{\omega_{vm}(q, a, b, P_r^2, \langle \delta P^2 \rangle)} \frac{d\mathbf{q}}{(2\pi)^3}, \quad (10)$$

where the energy spectrum of the collective vector mode $\hbar \omega_{vm}(q, a, b, P_r^2, \langle \delta P^2 \rangle) = \hbar \sqrt{\Delta^2(a, b, P_r^2, \langle \delta P^2 \rangle) + gq^2/m_p}$ with the excitation gap $\Delta(a, b, P_r^2, \langle \delta P^2 \rangle)$ given in Eq. (6). The polarization fluctuation here consists of the contributions from the zero-point oscillation and thermal excitation in the Bosonic excitation of the collective vector mode. We next introduce the proposed renormalization process shown in Fig. 1.

Renormalization by zero-point fluctuations.—At zero temperature, one can summarize Eqs. (4) and (5) as well as Eqs. (10) and (6), and directly find the self-consistent renormalization processes by the zero-point fluctuations:

$$a_0 = a + b(2/d_p + 1) \langle \delta P_{z0}^2 \rangle + \lambda(4/d_p + 1) (\langle \delta P_{z0}^2 \rangle)^2, \quad (11)$$

$$b_0 = b + 2\lambda(4/d_p + 1) \langle \delta P_{z0}^2 \rangle, \quad (12)$$

where the zero-point fluctuations:

$$\langle \delta P_{z0}^2 \rangle = \int \frac{\hbar}{2m_p} \frac{1}{\omega_{vm}(q, a, b, P_0^2, \langle \delta P_{z0}^2 \rangle)} \frac{d\mathbf{q}}{(2\pi)^3}, \quad (13)$$

and the zero-temperature long-range ordered polarization: $P_0^2 = (-b_0 + \sqrt{b_0^2 - 4\lambda a_0}) / (2\lambda)$ for $a_0 < 0$ and $P_0^2 = 0$ for $a_0 > 0$.

Renormalization by thermal fluctuations.—After the renormalization processes by the zero-point fluctuations, according to Fig. 1, the self-consistent renormalization processes by the thermal fluctuations at finite temperatures are given by

$$\alpha = a_0 + b_0(2/d_p + 1) \langle \delta P_{\text{th}}^2(T) \rangle + \lambda(4/d_p + 1) (\langle \delta P_{\text{th}}^2(T) \rangle)^2 + \delta \alpha(T), \quad (14)$$

$$\beta = b_0 + 2\lambda(4/d_p + 1) \langle \delta P_{\text{th}}^2(T) \rangle, \quad (15)$$

where the thermal fluctuations are determined by subtracting the zero-temperature part from Eq. (10) and are written as

$$\langle \delta P_{\text{th}}^2 \rangle = \int \frac{\hbar}{2m_p} \left\{ \frac{\coth[\hbar \omega_{vm}(q, a_0, b_0, P_r^2, \langle \delta P_{\text{th}}^2 \rangle) / (2k_B T)]}{\omega_{vm}(q, a_0, b_0, P_r^2, \langle \delta P_{\text{th}}^2 \rangle)} - \frac{1}{\omega_{vm}(q, a_0, b_0, P_0^2, 0)} \right\} \frac{d\mathbf{q}}{(2\pi)^3}, \quad (16)$$

and finite-temperature long-range ordered polarization: $P_r^2 = (-\beta + \sqrt{\beta^2 - 4\lambda\alpha})/(2\lambda)$ for $\alpha < 0$ and $P_r^2 = 0$ for $\alpha > 0$. We have introduced a correction/perturbation term $\delta\alpha(T)$ in Eq. (14), which can account for the coupling of the polarization field with the gapless acoustic phonons (i.e., thermal expansion) through the electrostrictive effect or take account into the structural instabilities due to lattice vibration caused by the excitation of the collective vector mode (see Supplementary Materials).

It should be emphasized that the proposed collective vector mode here is a direct and physically fundamental consequence of the quasiparticle excitation that emerges after the condensation of the imaginary-frequency phonons, which has long been overlooked in the literature and becomes an exclusive hidden excitation. In fact, in the quantum paraelectrics SrTiO₃ and KTaO₃, if the dielectric properties are governed by the soft phonons [78] (remaining real-frequency phonons on the unstable-phonon branch) rather than the collective vector mode, the inverse dielectric function should be insensitive to the temperature variation below $T_{\text{op}} = \hbar\Delta_{\text{op}}/k_B$ (24 K for SrTiO₃ and 36 K for KTaO₃ [22, 79–81]) due to the minimal excitation of the soft phonons (with frequencies $\omega_{\text{op}} = \sqrt{\Delta_{\text{op}}^2 + v_{\text{op}}^2 q^2}$), but this is strongly against the experimental findings of the non-classical T -square behaviors [22] that are shown in Figs. 2 and 3. In this situation, the collective vector mode with a nearly vanishing excitation gap naturally resolves this issue. In fact, in a recent pump-probe optical experiment performed in KTaO₃ [82], from the Fourier transform of the time-resolved second harmonic generation signal, it is found that at temperatures below 40 K, besides the widely reported single mode that emerges at 1.8 THz, there exists another mode at lower frequency of 0.4 THz. The 1.8 THz mode corresponds to the second-order excitation of the widely reported soft-phonon mode by resonant excitation, and its frequency $\Delta_{\text{op}} \approx 0.9$ THz (~ 3.7 meV ~ 43 K) determined from this optical experiment by $2\Delta_{\text{op}} = 1.8$ THz agrees with the one ($\hbar\Delta_{\text{op}}/k_B = 36$ K) measured from the Raman scattering experiments at 4 K [79, 80]. The observed 0.4 THz mode, should correspond to the linear-order excitation of the proposed collective vector mode here, by three-phonon interactions with the optical soft phonons, and its frequency $\Delta \approx 0.4$ THz (~ 1.65 meV) determined from this optical experiment is very close to the predicted one $\hbar\Delta = \hbar\sqrt{a_0/m_p} \approx 1.54$ meV from the present theory. This experiment should directly demonstrate the existence of the collective vector mode, which has long been overlooked in the literature.

-
- [1] A. A. Abrikosov, L. P. Gorkov, and I. E. Dzyaloshinski, *Methods of quantum field theory in statistical physics* (Prentice Hall, Englewood Cliffs, 1963).
- [2] Y. Nambu, Nobel Lecture: Spontaneous symmetry breaking in particle physics: A case of cross fertilization, *Rev. Mod. Phys.* **81**, 1015 (2009).
- [3] D. Pekker and C. Varma, Amplitude/Higgs modes in condensed matter physics, *Annu. Rev. Condens. Matter Phys.* **6**, 269 (2015).
- [4] P. W. Higgs, Broken symmetries and the masses of gauge bosons, *Phys. Rev. Lett.* **13**, 508 (1964).
- [5] F. Englert and R. Brout, Broken symmetry and the mass of gauge vector mesons, *Phys. Rev. Lett.* **13**, 321 (1964).
- [6] R. Matsunaga, Y. I. Hamada, K. Makise, Y. Uzawa, H. Terai, Z. Wang, and R. Shimano, Higgs amplitude mode in the BCS superconductors Nb_{1-x}Ti_xN induced by terahertz pulse excitation, *Phys. Rev. Lett.* **111**, 057002 (2013).
- [7] R. Matsunaga, N. Tsuji, H. Fujita, A. Sugioka, K. Makise, Y. Uzawa, H. Terai, Z. Wang, H. Aoki, and R. Shimano, Light-induced collective pseudospin precession resonating with Higgs mode in a superconductor, *Science* **345**, 1145 (2014).
- [8] F. Yang and M. Wu, Gauge-invariant microscopic kinetic theory of superconductivity: Application to the optical response of Nambu-Goldstone and Higgs modes, *Phys. Rev. B* **100**, 104513 (2019).
- [9] R. Shimano and N. Tsuji, Higgs mode in superconductors, *Annu. Rev. Condens. Matter Phys.* **11**, 103 (2020).
- [10] H. Chu, M.-J. Kim, K. Katsumi, S. Kovalev, R. D. Dawson, L. Schwarz, N. Yoshikawa, G. Kim, D. Putzky, Z. Z. Li, *et al.*, Phase-resolved Higgs response in superconducting cuprates, *Nat. Commun.* **11**, 1793 (2020).
- [11] F. Yang and M. Wu, Theory of Higgs modes in d-wave superconductors, *Phys. Rev. B* **102**, 014511 (2020).
- [12] L. Pollet and N. Prokof'ev, Higgs mode in a two-dimensional superfluid, *Phys. Rev. Lett.* **109**, 010401 (2012).
- [13] M. Endres, T. Fukuhara, D. Pekker, M. Cheneau, P. Schauß, C. Gross, E. Demler, S. Kuhr, and I. Bloch, The 'Higgs' amplitude mode at the two-dimensional superfluid/Mott insulator transition, *Nature* **487**, 454 (2012).
- [14] C. Rüegg, B. Normand, M. Matsumoto, A. Furrer, D. F. McMorrow, K. W. Krämer, H.-U. Güdel, S. N. Gvasaliya, H. Mutka, and M. Boehm, Quantum magnets under pressure: controlling elementary excitations in TiCuCl₃, *Phys. Rev. Lett.* **100**, 205701 (2008).
- [15] A. Jain, M. Krautloher, J. Porras, G. Ryu, D. Chen, D. Abernathy, J. Park, A. Ivanov, J. Chaloupka, G. Khaliullin, *et al.*, Higgs mode and its decay in a two-dimensional antiferromagnet, *Nat. Phys.* **13**, 633 (2017).
- [16] T. Hong, M. Matsumoto, Y. Qiu, W. Chen, T. R. Gentile, S. Watson, F. F. Awwadi, M. M. Turnbull, S. E. Dissanayake, H. Agrawal, *et al.*, Higgs amplitude mode in a two-dimensional quantum antiferromagnet near the quantum critical point, *Nat. Phys.* **13**, 638 (2017).
- [17] N. Yoshikawa, H. Suganuma, H. Matsuoka, Y. Tanaka, P. Hemme, M. Cazayous, Y. Gallais, M. Nakano, Y. Iwasa, and R. Shimano, Ultrafast switching to an insulating-like metastable state by amplitudon excitation of a charge density wave, *Nat. Phys.* **17**, 909 (2021).
- [18] S. Sugai, Y. Takayanagi, and N. Hayamizu, Phason and Amplitudon in the charge-density-wave phase of one-dimensional charge stripes in La_{2-x}Sr_xCuO₄, *Phys. Rev. Lett.* **96**, 137003 (2006).
- [19] D. H. Torchinsky, F. Mahmood, A. T. Bollinger, I. Božović, and N. Gedik, Fluctuating charge-density waves in a cuprate superconductor, *Nat. Mater.* **12**, 387 (2013).
- [20] P. Tang, R. Iguchi, K.-i. Uchida, and G. E. Bauer, Excitations of the ferroelectric order, *Phys. Rev. B* **106**, L081105 (2022).

- [21] P. Coleman, *Introduction to many-body physics* (Cambridge University Press, 2015).
- [22] S. Rowley, L. Spalek, R. Smith, M. Dean, M. Itoh, J. Scott, G. Lonzarich, and S. Saxena, Ferroelectric quantum criticality, *Nat. Phys.* **10**, 367 (2014).
- [23] G. Conduit and B. Simons, Theory of quantum paraelectrics and the metaelectric transition, *Phys. Rev. B* **81**, 024102 (2010).
- [24] R. Roussev and A. Millis, Theory of the quantum paraelectric-ferroelectric transition, *Phys. Rev. B* **67**, 014105 (2003).
- [25] L. Palova, P. Chandra, and P. Coleman, Quantum critical paraelectrics and the Casimir effect in time, *Phys. Rev. B* **79**, 075101 (2009).
- [26] B. Silverman and R. Joseph, Temperature dependence of the dielectric constant of paraelectric materials, *Phys. Rev.* **129**, 2062 (1963).
- [27] M. E. Lines and A. M. Glass, *Principles and applications of ferroelectrics and related materials* (Oxford University press, 2001).
- [28] H. Fujishita, S. Kitazawa, M. Saito, R. Ishisaka, H. Okamoto, and T. Yamaguchi, Quantum paraelectric states in SrTiO₃ and KTaO₃: Barrett model, Vendik model, and quantum criticality, *J. Phys. Soc. Jpn.* **85**, 074703 (2016).
- [29] E. Tadmor, U. Waghmare, G. Smith, and E. Kaxiras, Polarization switching in PbTiO₃: an ab initio finite element simulation, *Acta Mater.* **50**, 2989 (2002).
- [30] W. Zhong, D. Vanderbilt, and K. Rabe, Phase transitions in BaTiO₃ from first principles, *Phys. Rev. Lett.* **73**, 1861 (1994).
- [31] W. Zhong, D. Vanderbilt, and K. Rabe, First-principles theory of ferroelectric phase transitions for perovskites: The case of BaTiO₃, *Phys. Rev. B* **52**, 6301 (1995).
- [32] U. Waghmare and K. Rabe, Ab initio statistical mechanics of the ferroelectric phase transition in PbTiO₃, *Phys. Rev. B* **55**, 6161 (1997).
- [33] L. Bellaiche, A. García, and D. Vanderbilt, Finite-temperature properties of Pb(Zr_{1-x}Ti_x)O₃ alloys from first principles, *Phys. Rev. Lett.* **84**, 5427 (2000).
- [34] I. I. Naumov, L. Bellaiche, and H. Fu, Unusual phase transitions in ferroelectric nanodisks and nanorods, *Nature* **432**, 737 (2004).
- [35] I. A. Kornev, L. Bellaiche, P.-E. Janolin, B. Dkhil, and E. Suard, Phase diagram of Pb(Zr,Ti)O₃ solid solutions from first principles, *Phys. Rev. Lett.* **97**, 157601 (2006).
- [36] A. Akbarzadeh, S. Prosandeev, E. J. Walter, A. Al-Barakaty, and L. Bellaiche, Finite-temperature properties of Ba(Zr,Ti)O₃ relaxors from first principles, *Phys. Rev. Lett.* **108**, 257601 (2012).
- [37] P. S. H. Ghosez, X. Gonze, and J.-P. Michenaud, Ab initio phonon dispersion curves and interatomic force constants of barium titanate, *Ferroelectrics* **206**, 205 (1998).
- [38] R. E. Cohen, Origin of ferroelectricity in perovskite oxides, *Nature* **358**, 136 (1992).
- [39] X. He, D. Bansal, B. Winn, S. Chi, L. Boatner, and O. Delaire, Anharmonic eigenvectors and acoustic phonon disappearance in quantum paraelectric SrTiO₃, *Phys. Rev. Lett.* **124**, 145901 (2020).
- [40] C. Verdi, L. Ranalli, C. Franchini, and G. Kresse, Quantum paraelectricity and structural phase transitions in strontium titanate beyond density functional theory, *Phys. Rev. Mater.* **7**, L030801 (2023).
- [41] Y. Qi, S. Liu, I. Grinberg, and A. M. Rappe, Atomistic description for temperature-driven phase transitions in BaTiO₃, *Phys. Rev. B* **94**, 134308 (2016).
- [42] L. Gigli, A. Goscinski, M. Ceriotti, and G. A. Tribello, Modeling the ferroelectric phase transition in barium titanate with DFT accuracy and converged sampling, *Phys. Rev. B* **110**, 024101 (2024).
- [43] H. Wu, R. He, Y. Lu, and Z. Zhong, Large-scale atomistic simulation of quantum effects in SrTiO₃ from first principles, *Phys. Rev. B* **106**, 224102 (2022).
- [44] A. Devonshire, Theory of ferroelectrics, *Adv. Phys.* **3**, 85 (1954).
- [45] M. Haun, Z. Zhuang, E. Furman, S. Jang, and L. E. Cross, Thermodynamic theory of the lead zirconate-titanate solid solution system, part III: Curie constant and sixth-order polarization interaction dielectric stiffness coefficients, *Ferroelectrics* **99**, 45 (1989).
- [46] M. J. Haun, E. Furman, S. Jang, H. McKinstry, and L. Cross, Thermodynamic theory of PbTiO₃, *J. Appl. Phys.* **62**, 3331 (1987).
- [47] L. Chen, V. Nagarajan, R. Ramesh, and A. Roytburd, Nonlinear electric field dependence of piezoresponse in epitaxial ferroelectric lead zirconate titanate thin films, *J. Appl. Phys.* **94**, 5147 (2003).
- [48] W. Cochran, Soft modes, a personal perspective, *Ferroelectrics* **35**, 3 (1981).
- [49] W. Cochran, Crystal stability and the theory of ferroelectricity part II. Piezoelectric crystals, *Adv. Phys.* **10**, 401 (1961).
- [50] W. Yelon, W. Cochran, G. Shirane, and A. Linz, Neutron scattering study of the soft modes in cubic potassium tantalate-niobate, *Ferroelectrics* **2**, 261 (1971).
- [51] R. A. Cowley, The phase transition of strontium titanate, *Philos. Transact. A Math. Phys. Eng. Sci.* **354**, 2799 (1996).
- [52] R. Cowley, On the theory of ferroelectricity and anharmonic effects in crystals, *Phil. Mag.* **11**, 673 (1965).
- [53] W. Cochran, Dynamical, scattering and dielectric properties of ferroelectric crystals, *Adv. Phys.* **18**, 157 (1969).
- [54] W. Cochran, Crystal stability and the theory of ferroelectricity, *Adv. Phys.* **9**, 387 (1960).
- [55] P. Lee, T. Rice, and P. Anderson, Conductivity from charge or spin density waves, *Solid State Commun.* **14**, 703 (1974).
- [56] M. E. Peskin, *An introduction to quantum field theory* (CRC press, 2018).
- [57] E. Matsushita and S. Segawa, A model of quantum paraelectric-ferroelectric transition, *Ferroelectrics* **347**, 1 (2007).
- [58] X. Li, T. Qiu, J. Zhang, E. Baldini, J. Lu, A. M. Rappe, and K. A. Nelson, Terahertz field-induced ferroelectricity in quantum paraelectric SrTiO₃, *Science* **364**, 1079 (2019).
- [59] B. Cheng, P. L. Kramer, Z.-X. Shen, and M. C. Hoffmann, Terahertz-driven local dipolar correlation in a quantum paraelectric, *Phys. Rev. Lett.* **130**, 126902 (2023).
- [60] D. J. Singh, Stability and phonons of KTaO₃, *Phys. Rev. B* **53**, 176 (1996).
- [61] G. Shirane and Y. Yamada, Lattice-dynamical study of the 110 K phase transition in SrTiO₃, *Phys. Rev.* **177**, 858 (1969).
- [62] H. Vogt, Refined treatment of the model of linearly coupled anharmonic oscillators and its application to the temperature dependence of the zone-center soft-mode frequencies of KTaO₃ and SrTiO₃, *Phys. Rev. B* **51**, 8046 (1995).
- [63] A. Beattie and G. Samara, Pressure dependence of the elastic constants of SrTiO₃, *J. Appl. Phys.* **42**, 2376 (1971).
- [64] Q. Tao, B. Loret, B. Xu, X. Yang, C. W. Rischau, X. Lin, B. Fauqué, M. J. Verstraete, and K. Behnia, Nonmonotonic anisotropy in charge conduction induced by antiferrodistortive transition in metallic SrTiO₃, *Phys. Rev. B* **94**, 035111 (2016).
- [65] K. A. Müller and H. Burkard, SrTiO₃: An intrinsic quantum paraelectric below 4 K, *Phys. Rev. B* **19**, 3593 (1979).
- [66] S. Wemple, Some transport properties of oxygen-deficient single-crystal potassium tantalate (KTaO₃), *Phys. Rev.* **137**, A1575 (1965).
- [67] W. Abel, Effect of pressure on the static dielectric constant of KTaO₃, *Phys. Rev. B* **4**, 2696 (1971).

- [68] C. Ang, A. Bhalla, and L. Cross, Dielectric behavior of paraelectric KTaO_3 , CaTiO_3 , and $(\text{Ln}_{1/2}\text{Na}_{1/2})\text{TiO}_3$ under a dc electric field, *Phys. Rev. B* **64**, 184104 (2001).
- [69] O. Aktas, S. Crossley, M. A. Carpenter, and E. K. Salje, Polar correlations and defect-induced ferroelectricity in cryogenic KTaO_3 , *Phys. Rev. B* **90**, 165309 (2014).
- [70] Z. Yang, D. Lee, J. Yue, J. Gabel, T.-L. Lee, R. D. James, S. A. Chambers, and B. Jalan, Epitaxial SrTiO_3 films with dielectric constants exceeding 25,000, *Proc. Natl. Acad. Sci.* **119**, e2202189119 (2022).
- [71] D. Khmel'nitskii and V. Shneerson, Phase-transition of displacement type in crystals at very low temperatures, *Zh. Eksp. Teor. Fiz* **64**, 316 (1973).
- [72] G. Samara, Pressure and temperature dependence of the dielectric properties and phase transitions of the ferroelectric perovskites: PbTiO_3 and BaTiO_3 , *Ferroelectrics* **2**, 277 (1971).
- [73] J. Remeika and A. Glass, The growth and ferroelectric properties of high resistivity single crystals of lead titanate, *Mater. Res. Bull.* **5**, 37 (1970).
- [74] S. Ikegami, I. Ueda, and T. Nagata, Electromechanical properties of PbTiO_3 ceramics containing La and Mn, *J. Acoust. Soc. Am.* **50**, 1060 (1971).
- [75] B. Tuttle, D. Payne, and J. Mukherjee, Ferroelectric materials for dielectric power conversion, *Ferroelectrics* **27**, 219 (1980).
- [76] F. Yang and L.-Q. Chen, Thermodynamic theory of disordered 2D superconductors, arXiv:2410.05216 (2024).
- [77] L. Landau, E. Lifshitz, and L. E. Reichl, *Statistical physics, part I* (American Institute of Physics, 1981).
- [78] A. Sirenko, C. Bernhard, A. Golnik, A. M. Clark, J. Hao, W. Si, and X. Xi, Soft-mode hardening in SrTiO_3 thin films, *Nature* **404**, 373 (2000).
- [79] G. Shirane, R. Nathans, and V. Minkiewicz, Temperature dependence of the soft ferroelectric mode in KTaO_3 , *Phys. Rev.* **157**, 396 (1967).
- [80] P. Fleury and J. Worlock, Electric-field-induced raman scattering in SrTiO_3 and KTaO_3 , *Phys. Rev.* **174**, 613 (1968).
- [81] Y. Yamada and G. Shirane, Neutron scattering and nature of the soft optical phonon in SrTiO_3 , *J. Phys. Soc. Jpn.* **26**, 396 (1969).
- [82] F. Yang, X. J. Li, and C. L. Q. (in preparation).

Microscopic theory of displacive ferroelectricity: applications to quantum criticality and classical phase transitions (Supplement material)

F. Yang^{1,*} and L. Q. Chen^{1,†}

¹*Department of Materials Science and Engineering and Materials Research Institute,
The Pennsylvania State University, University Park, PA 16802, USA*

Derivation of the developed theory within fundamental path-integral approach in Matsubara representation

For checking the self-consistency of our proposed microscopic thermodynamic theory, below we present a separate framework to derive the same theory using the fundamental path-integral approach in the Matsubara (imaginary-time) representation. This derivation leads to the same theoretical description as the one in the Methods section of the main text, which is derived by using the fluctuation dissipation theorem via introducing a thermal field. Specifically, with the Lagrangian of the polarization field in Eq. (7) in the main text, the action in the Matsubara representation is written as

$$S = \int_0^{\hbar/(k_B T)} d\tau d\mathbf{q} \left[\frac{m_p}{2} (\partial_\tau \delta P)^2 + \frac{gq^2}{2} \delta P^2 + \frac{a}{2} \delta P^2 + \frac{b}{4} \delta P^4 + \frac{\lambda}{6} \delta P^6 + \frac{b}{2} \left(\frac{2}{d_p} + 1 \right) P_r^2 \delta P^2 + \frac{\lambda}{2} \left(\frac{4}{d_p} + 1 \right) (P_r^4 \delta P^2 + P_r^2 \delta P^4) \right] + S_G, \quad (S1)$$

with $S_G = \frac{a}{2} P_r^2 + \frac{b}{4} P_r^4 + \frac{\lambda}{6} P_r^6$. To obtain the effective action (partial function) of the long-range ordered polarization P_r^2 , one can perform the standard integration over the bosonic field of the polarization fluctuation δP within the path-integral formalism. However, to tackle the phase transition, it requires formulating the infinite-order perturbation expansions of the self-energy correction due to the coupling between the polarization fluctuation and long-range ordered polarization, or picking up the appropriate diagrammatic representation in a self-consistent way, making it a challenging problem. Here we present two self-consistent methods similar to the treatments of superconductors [1–5].

Generating functional methods.—Within the path-integral formalism, using the action in Eq. (S1), the thermal average of the polarization fluctuation can be written as [5, 6]

$$\begin{aligned} \langle \delta P^2 \rangle &= \int \frac{d\mathbf{q}}{(2\pi)^3} \left\langle \left| \delta P(\tau, \mathbf{q}) \delta P(\tau, -\mathbf{q}) e^{-\frac{S}{\hbar}} \right| \right\rangle = \int \frac{d\mathbf{q}}{(2\pi)^3} \int \frac{D\delta P}{\mathcal{Z}_0} \left[\delta P(\tau, \mathbf{q}) \delta P(\tau, -\mathbf{q}) e^{-\frac{S}{\hbar}} \right] \\ &= \int \frac{d\mathbf{q}}{(2\pi)^3} \int \frac{D\delta P}{\mathcal{Z}_0} \delta J_{\mathbf{q}} \delta J_{-\mathbf{q}} \left\{ e^{-\frac{S}{\hbar} - \int_0^{\hbar/k_B T} d\tau d\mathbf{q}' [J_{\mathbf{q}'} \delta P(\tau, \mathbf{q}')] } \right\} \Big|_{J=0} \\ &= \int \frac{d\mathbf{q}}{(2\pi)^3} \int \frac{D\delta P}{\mathcal{Z}_0} e^{-\frac{S_G}{\hbar}} \delta J_{\mathbf{q}}^2 \left\{ e^{-\int_0^{\hbar/k_B T} d\tau d\mathbf{q}' \left\{ \frac{1}{\hbar} \delta P(\tau, \mathbf{q}') [m_p \omega_{vm}^2(q', a, b, P_r^2, \langle \delta P^2 \rangle) - m_p \partial_\tau^2] \delta P(\tau, \mathbf{q}') + J_{\mathbf{q}'} \delta P(\tau, \mathbf{q}') \right\}} \right\} \Big|_{J=0} \\ &= \int \frac{d\mathbf{q}}{(2\pi)^3} \delta J_{\mathbf{q}}^2 \exp \left\{ \int_0^{\hbar/(k_B T)} d\tau d\mathbf{q}' \left[\frac{1}{2} J_{\mathbf{q}'} \frac{\hbar}{m_p \omega_{vm}^2(q', a, b, P_r^2, \langle \delta P^2 \rangle) - m_p \partial_\tau^2} J_{\mathbf{q}'} \right] \right\} \Big|_{J=J^*=0} \\ &= - \int \frac{d\mathbf{q}}{(2\pi)^3} \frac{k_B T}{\hbar} \sum_n \frac{\hbar/m_p}{(i\omega_n)^2 - \omega_{vm}^2(q, a, b, P_r^2, \langle \delta P^2 \rangle)} = \int \frac{d\mathbf{q}}{(2\pi)^3} \frac{\hbar}{m_p} \frac{\coth[\hbar\omega_{vm}(q, a, b, P_r^2, \langle \delta P^2 \rangle)/(2k_B T)]}{2\omega_{vm}(q, a, b, P_r^2, \langle \delta P^2 \rangle)}. \quad (S2) \end{aligned}$$

Here, we utilized the mean-field approximation [i.e., variation with respect to δP^2] to obtain the thermally averaged ω_{vm}^2 ; $\omega_n = 2n\pi k_B T/\hbar$ represents the bosonic Matsubara frequencies; $J_{\mathbf{q}}$ denotes the generating functional and $\delta J_{\mathbf{q}}$ stands for the functional derivative [6, 7]; $\mathcal{Z}_0 = \langle |e^{-S}| \rangle$ is the normalization factor. Consequently, Eq. (10) in the main text is derived. Then, substituting Eq. (S2) to the action in Eq. (S1) and extracting the thermally averaged contributions from P_r^2 afterwards, one finds the partial function (i.e., free energy) of the long-range ordered polarization.

Self-consistent Green function methods.—We re-write the action in Eq. (S1) as

$$S = \int_0^{\hbar/(k_B T)} d\tau d\mathbf{q} \frac{1}{2} \delta P(\tau, \mathbf{q}) D_{vm}^{-1}(\partial_\tau, q) \delta P(\tau, \mathbf{q}) + S_G, \quad (S3)$$

where the inverse Green function is defined as [5, 6]

$$D_{vm}^{-1}(\partial_\tau, q) = gq^2 + a + b\delta P^2/2 + \lambda\delta P^4/3 + b(2/d_p + 1)P_r^2 + \lambda(4/d_p + 1)(P_r^4 + P_r^2\delta P^2) - m_p\partial_\tau^2. \quad (S4)$$

It is noted that here we have kept the coupling between the polarization fluctuation and long-range ordered polarization in the Green function rather than in the self-energy as in the conventional way. Then, performing the integration over the bosonic field

of the fluctuation within the path-integral formalism, one finds the effective action:

$$S_{\text{eff}} = \frac{1}{2} \hbar \bar{\text{Tr}} \ln [D_{vm}^{-1}(\partial_\tau, q)] + S_G. \quad (\text{S5})$$

Through the variation with respect to P_r , the equation to determine the long-range ordered polarization reads

$$\frac{1}{2} \hbar \bar{\text{Tr}} \left\{ \partial_{P_r} [D_{vm}^{-1}(\partial_\tau, q)] D_{vm}(\partial_\tau, q) \right\} + \partial_{P_r} S_G = 0. \quad (\text{S6})$$

Imposing the mean-field approximation on the thermal average, the above equation becomes

$$\begin{aligned} & \left\{ \hbar \bar{\text{Tr}} \left\{ \frac{b(2/d_p+1)P_r + \lambda(4/d_p+1)(2P_r^3 + P_r \delta P^2)}{gq^2 + a + b\delta P^2/2 + \lambda\delta P^4/3 + b(2/d_p+1)P_r^2 + \lambda(4/d_p+1)(P_r^4 + P_r^2 \delta P^2) - m_p \partial_\tau^2} \right\} \right\} + \partial_{P_r} S_G = 0 \\ \Rightarrow & \bar{\text{Tr}} \left\{ \frac{\hbar [b(2/d_p+1)P_r + \lambda(4/d_p+1)(2P_r^3 + P_r \delta P^2)] \delta P^2}{[gq^2 + a + b(2/d_p+1)P_r^2] \delta P^2 + b\delta P^4/2 + \lambda\delta P^6/3 + \lambda(4/d_p+1)(P_r^4 \delta P^2 + P_r^2 \delta P^4) - m_p \delta P \partial_\tau^2 \delta P} \right\} + \partial_{P_r} S_G = 0 \\ \Rightarrow & \int \frac{d\mathbf{q}}{(2\pi)^3} \sum_n \frac{k_B T [b(2/d_p+1)P_r + \lambda(4/d_p+1)(2P_r^3 + P_r \langle \delta P^2 \rangle)] \langle \delta P^2 \rangle}{\langle [gq^2 + a + b(2/d_p+1)P_r^2 - m_p (i\omega_n)^2] \delta P^2 + b\delta P^4/2 + \lambda\delta P^6/3 + \lambda(4/d_p+1)(P_r^4 \delta P^2 + P_r^2 \delta P^4) \rangle} + \partial_{P_r} S_G = 0 \\ \Rightarrow & \int \frac{d\mathbf{q}}{(2\pi)^3} \sum_n \frac{k_B T [b(2/d_p+1)P_r + \lambda(4/d_p+1)(2P_r^3 + P_r \langle \delta P^2 \rangle)] \langle \delta P^2 \rangle}{[\omega_{vm}^2(q, a, b, P_r^2, \langle \delta P^2 \rangle) - (i\omega_n)^2] \langle \delta P^2 \rangle} + \partial_{P_r} S_G = 0 \\ \Rightarrow & [b(2/d_p+1)P_r + \lambda(4/d_p+1)(2P_r^3 + P_r \langle \delta P^2 \rangle)] \int \frac{d\mathbf{q}}{(2\pi)^3} \sum_n \frac{k_B T / m_p}{\omega_{vm}^2(q, a, b, P_r^2, \langle \delta P^2 \rangle) - (i\omega_n)^2} + aP_r + bP_r^3 + \lambda P_r^5 = 0 \\ \Rightarrow & [b(2/d_p+1)P_r + \lambda(4/d_p+1)(2P_r^3 + P_r \langle \delta P^2 \rangle)] \langle \delta P^2 \rangle + aP_r + bP_r^3 + \lambda P_r^5 = 0 \\ \Rightarrow & [a + b(2/d_p+1) \langle \delta P^2 \rangle + \lambda(4/d_p+1) (\langle \delta P^2 \rangle)^2] P_r + [b + 2\lambda(4/d_p+1) \langle \delta P^2 \rangle] P_r^3 + \lambda P_r^5 = 0, \end{aligned} \quad (\text{S7})$$

with

$$\langle \delta P^2 \rangle = \int \frac{d\mathbf{q}}{(2\pi)^3} \frac{k_B T}{\hbar} \sum_n \frac{\hbar / m_p}{\omega_{vm}^2(q, a, b, P_r^2, \langle \delta P^2 \rangle) - (i\omega_n)^2} = \int \frac{d\mathbf{q}}{(2\pi)^3} \frac{\hbar}{m_p} \frac{\coth [\hbar \omega_{vm}(q, a, b, P_r^2, \langle \delta P^2 \rangle) / (2k_B T)]}{2\omega_{vm}(q, a, b, P_r^2, \langle \delta P^2 \rangle)}. \quad (\text{S8})$$

Here, we have taken the variation with respect to δP^2 to obtain thermally averaged ω_{vm}^2 in consideration of the mean-field approximation. Consequently, the thermally averaged fluctuation [Eq. (10) in the main text] and the equation to determine the long-range ordered polarization [i.e., free-energy parameters in Eqs. (4) and (5) in the main text] are derived.

Correction of acoustic phonon in quantum paraelectrics SrTiO₃ and KTaO₃

In the quantum paraelectrics with a nearly vanishing a_0 , the correction due to the coupling of the polarization field with the gapless acoustic phonons through the electrostrictive effect, which should manifest with the characteristic features at low temperatures, becomes inevitable because of the small $1/\varepsilon$ at low-temperature limit. In this part, we introduce a model to include this coupling [8–10] and its correction to the renormalization processes. Specifically, the electrostrictive effect originates from the three-phonon interactions between two optical phonons and one acoustic phonon, and results in a coupling between the long-range ordered polarization and strain s_i (voigt notation) [11]. This coupling energy in cubic perovskites reads $E_{\text{int}} = -C \sum_{i=1,2,3} s_i P^2$ with $C > 0$ being the cubic electrostrictive constant. By adding this coupling contribution to the free energy of the long-range ordered polarization, one directly finds a thermally averaged correction [in Eq. (14) in the main text]:

$$\delta\alpha = -C \langle s \rangle, \quad (\text{S9})$$

where $\langle s \rangle = \langle s_1 \rangle = \langle s_2 \rangle = \langle s_3 \rangle$ (cubic perovskite), and this thermal average within the quantum statistic theory of the acoustic phonon is given by

$$\langle s \rangle = - \sum_\lambda \frac{d_\lambda}{\rho v_\lambda^2} \int \frac{\hbar q^2 n_B(\hbar v_\lambda q)}{\rho} \frac{d\mathbf{q}}{2v_\lambda q (2\pi)^3}. \quad (\text{S10})$$

Here, ρ stands for the mass density; v_λ denotes the group velocity of the λ -branch (LA, TA) acoustic phonon; $n_B(\hbar\omega)$ represents the Bose-Einstein distribution; $d_\lambda < 0$ represents the contribution coefficient from the λ -branch acoustic phonon to the thermal

expansion, which is related to the third-order non-harmonic coefficient of the strain. Consequently, by adding the contributions from the above equations in the self-consistent formulation of the renormalization processes by the thermal fluctuations, the coupling effect of the polarization field with acoustic phonons via electrostrictive effect is incorporated in the our thermodynamic theory.

Detailed derivations.—We next present the detailed derivations of Eq. (S10). We start from the Lagrangian of the strain (i.e., acoustic phonons):

$$\mathcal{L}_s = \frac{1}{2}\rho(\partial_t \mathbf{u}_{\text{LA}})^2 - \frac{1}{2}e_{\text{LA}}s_{\text{LA}}^2 - \frac{1}{3}d_{111}s_{\text{LA}}^3 - 3d_{144}s_{\text{LA}}s_{\text{TA}}^2 + \frac{1}{2}\rho(\partial_t \mathbf{u}_{\text{TA}})^2 - \frac{1}{2}e_{\text{TA}}s_{\text{TA}}^2 - \frac{1}{3}d_{444}s_{\text{TA}}^3 - 3d_{114}s_{\text{LA}}^2s_{\text{TA}}, \quad (\text{S11})$$

where \mathbf{u}_λ and s_λ denote the lattice vibration and corresponding strain contributed by the λ -branch acoustic phonon, respectively; e_λ and d_{ijk} are the second-order harmonic and third-order non-harmonic coefficients. Using the Euler-Lagrange equation of motion [6], one finds

$$D_{\text{LA}}^{-1}(t, \mathbf{q})s_{\text{LA}} = \sigma_{\text{LA}}(t, \mathbf{q}) - d_{111}s_{\text{LA}}^2 - 3d_{144}s_{\text{TA}}^2 - 6d_{114}s_{\text{LA}}s_{\text{TA}}, \quad (\text{S12})$$

$$D_{\text{TA}}^{-1}(t, \mathbf{q})s_{\text{TA}} = \sigma_{\text{TA}}(t, \mathbf{q}) - d_{444}s_{\text{TA}}^2 - 3d_{114}s_{\text{LA}}^2 - 6d_{144}s_{\text{TA}}s_{\text{LA}}, \quad (\text{S13})$$

where the inverse Green function $D_\lambda^{-1}(t, \mathbf{q}) = (\rho/q^2)\partial_t^2 + e_\lambda + \gamma\partial_t$ with $\gamma = 0^+$ being the damping rate [5]. Here, we have introduced the thermal field $\sigma_\lambda(t, \mathbf{q})$ which obeys the fluctuation-dissipation theorem [12, 13]:

$$\langle \sigma_\lambda(\omega, \mathbf{q}) \sigma_{\lambda'}^*(\omega', \mathbf{q}') \rangle = \frac{\gamma \hbar \omega (2\pi)^4 \delta(\omega - \omega') \delta(\mathbf{q} - \mathbf{q}')}{\tanh[\hbar\omega/(2k_B T)]} \delta_{\lambda, \lambda'}. \quad (\text{S14})$$

From Eqs. (S12) and (S13), keeping the leading terms, one has

$$s_{\text{LA}} = D_{\text{LA}}\sigma_{\text{LA}} - d_{111}D_{\text{LA}}(D_{\text{LA}}\sigma_{\text{LA}})^2 - 3d_{144}D_{\text{LA}}(D_{\text{TA}}\sigma_{\text{TA}})^2 - 6d_{114}D_{\text{LA}}(D_{\text{LA}}\sigma_{\text{LA}})(D_{\text{TA}}\sigma_{\text{TA}}). \quad (\text{S15})$$

Consequently, with Eq. (S14), the thermal average is derived as

$$\langle s_{\text{LA}} \rangle = -\frac{d_{111}}{e_{\text{LA}}} \int \frac{\hbar q^2 n_B(\hbar q \sqrt{e_{\text{LA}}/\rho})}{\rho} \frac{d\mathbf{q}}{2q\sqrt{e_{\text{LA}}/\rho}} \frac{d\mathbf{q}}{(2\pi)^3} - \frac{3d_{144}}{e_{\text{TA}}} \int \frac{\hbar q^2 n_B(\hbar q \sqrt{e_{\text{TA}}/\rho})}{\rho} \frac{d\mathbf{q}}{2q\sqrt{e_{\text{TA}}/\rho}} \frac{d\mathbf{q}}{(2\pi)^3}. \quad (\text{S16})$$

Here, we have neglected the zero-point oscillations of the acoustic phonons. Considering the group velocity of the λ -branch acoustic phonon $v_\lambda = \sqrt{e_\lambda/\rho}$ and $\langle s_{\text{LA}} \rangle = \langle s_1 \rangle = \langle s \rangle$ for the cubic perovskite, one arrives at Eq. (S10).

Temperature dependence of inverse dielectric function in quantum paraelectrics

In this part, we present an analytical analysis of the temperature dependence of the inverse dielectric function in the quantum paraelectrics. In the quantum paraelectrics SrTiO₃ and KTaO₃, as the inverse dielectric function $1/\varepsilon(T) \propto \alpha(T)$, from Eq. (14) in the main text, one finds

$$1/\varepsilon(T) \propto a_0 + 4b_0 \langle \delta P_{\text{th}}^2 \rangle + \delta\alpha. \quad (\text{S17})$$

At low temperatures near zero, due to the gapped collective vector mode and hence minimum $\langle \delta P_{\text{th}}^2 \rangle$, the temperature variation of $1/\varepsilon(T)$ is dominated by the correction term $\delta\alpha$, i.e, the thermal expansion associated with the gapless acoustic phonon via the electrostrictive effect. It therefore decreases with the increase of temperature according to Eq. (S9).

With further increase in temperature, the increased thermal fluctuation from zero starts to dominate the temperature variation of $1/\varepsilon(T)$. In this situation, considering $P_r \equiv 0$ and nearly vanishing a_0 in quantum paraelectrics but neglecting the minimal $\langle \delta P_{\text{th}}^2 \rangle$ in the excitation gap Δ , from Eqs. (6) and (16) in the main text, one approximately has

$$\langle \delta P_{\text{th}}^2 \rangle \approx \int \frac{\hbar n_B(\hbar q \sqrt{g/m_p}) q^2 dq}{(2\pi)^2 m_p q \sqrt{g/m_p}} = \int \frac{\hbar n_B(\omega) \omega d\omega}{(2\pi)^2 m_p (g/m_p)^{3/2}} = -\sum_{n=1}^{\infty} \frac{\hbar (k_B T)^2 (1+nx) e^{-nx} \Big|_{x=0}^{x=\frac{\hbar\omega_c}{k_B T} \approx \infty}}{(2\pi)^2 n^2 m_p (g/m_p)^{3/2}} = \frac{\hbar (k_B T)^2 \zeta(2)}{(2\pi)^2 m_p (g/m_p)^{3/2}}, \quad (\text{S18})$$

leading to a non-classical T -square temperature behavior of the inverse dielectric function.

When the temperature increases to exceed $\hbar\omega_{vm}(q_c)/k_B$ at high temperatures, with q_c being the wave-vector cutoff, one approximately has

$$\langle \delta P_{\text{th}}^2 \rangle \approx k_B T \int_0^{q_c} \frac{\hbar q^2 dq / (2\pi)^2}{b_0 \langle \delta P_{\text{th}}^2 \rangle + g q^2} = k_B T \left[\sqrt{g q_c^2} - \sqrt{b_0 \langle \delta P_{\text{th}}^2 \rangle} \arctan \left(\sqrt{g q_c^2 / b_0 \langle \delta P_{\text{th}}^2 \rangle} \right) \right] \frac{\hbar}{(2\pi)^2 g^{3/2}}. \quad (\text{S19})$$

For SrTiO₃ and KTaO₃, $g q_c^2 / b_0 \langle \delta P_{\text{th}}^2 \rangle \approx 4g\varepsilon(T)q_c^2 \gg 1$, thereby leading to $\langle \delta P_{\text{th}}^2 \rangle \propto T$, and hence, the inverse dielectric function exhibits the classical linear- T (i.e., Curie-Weiss) behavior at high temperatures.

Model for ferroelectric PbTiO₃

We describe the theoretical model of the ferroelectric PbTiO₃ in this section. We take the ground-state Lagrangian of the polarization field limited by the crystal symmetry of PbTiO₃ [11]:

$$\begin{aligned} \mathcal{L} = & \frac{m_p}{2}(\partial_t \mathbf{P})^2 - \left[\frac{g}{2}(\nabla \mathbf{P})^2 + \frac{a_1}{2}(P_1^2 + P_2^2 + P_3^2) + \frac{a_{11}}{4}(P_1^4 + P_2^4 + P_3^4) + \frac{a_{111}}{6}(P_1^6 + P_2^6 + P_3^6) + a_{123}P_1^2P_2^2P_3^2 \right. \\ & \left. + a_{112}[P_1^4(P_2^2 + P_3^2) + P_2^4(P_1^2 + P_3^2) + P_3^4(P_1^2 + P_2^2)] + a_{12}(P_1^2P_2^2 + P_2^2P_3^2 + P_1^2P_3^2) \right]. \end{aligned} \quad (\text{S20})$$

Similarly, the polarization field $\mathbf{P} = \mathbf{P}_r + \delta \mathbf{P}$, consisting of the long-range ordered polarization $\mathbf{P}_r = P_r \mathbf{e}_3$ and polarization fluctuation $\delta \mathbf{P}$. Taking the angular average of the fluctuations by neglecting their odd orders, one has

$$\begin{aligned} \mathcal{L} = & \frac{m_p}{2}(\partial_t \delta P)^2 - \left[\frac{g}{2}(\nabla \delta P)^2 + \frac{a_1}{2}(P_r^2 + \delta P^2) + \frac{a_{11}}{4}\left(P_r^4 + \frac{\delta P^4}{3} + \frac{2P_r^2 \delta P^2}{3}\right) + \frac{a_{111}}{6}\left(P_r^6 + \frac{\delta P^6}{9} + P_r^4 \delta P^2 + \frac{P_r^2 \delta P^4}{3}\right) \right. \\ & \left. + a_{123}\left(\frac{\delta P^6}{27} + \frac{P_r^2 \delta P^4}{9}\right) + a_{112}\left(\frac{2\delta P^6}{9} + \frac{2P_r^4 \delta P^2}{3} + \frac{2P_r^2 \delta P^4}{3}\right) + a_{12}\left(\frac{\delta P^4}{3} + \frac{2\delta P^2 P_r^2}{3}\right) \right], \end{aligned} \quad (\text{S21})$$

where we have considered the isotropic fluctuations as an approximation. Consequently, the thermally averaged contributions purely from the long-range ordering in this Lagrangian gives rise to the free energy in Eq. (3) of the main text, and the corresponding free-energy parameters are written as

$$\alpha = a_1 + \left(\frac{a_{11}}{3} + \frac{4a_{12}}{3}\right)\langle \delta P^2 \rangle + \left(\frac{a_{111}}{9} + \frac{4a_{112}}{3} + \frac{2a_{123}}{9}\right)\langle \delta P^2 \rangle^2, \quad (\text{S22})$$

$$\beta = a_{11} + \left(\frac{2a_{111}}{3} + \frac{8a_{112}}{3}\right)\langle \delta P^2 \rangle, \quad (\text{S23})$$

$$\lambda = a_{111}. \quad (\text{S24})$$

Moreover, following the same way to derive Eq. (10) in the main text, by using the Euler-Lagrange equation of motion with respect to the polarization fluctuation from the Lagrangian in Eq. (S21) and employing the thermal field that obeys the fluctuation-dissipation theorem [12, 13], one can derive the thermally averaged polarization fluctuation:

$$\langle \delta P^2 \rangle = \int \frac{\hbar}{2m_p} \frac{\coth[\hbar\omega_{vm}^{\text{PTO}}(q, a_1, a_{11}, P_r^2, \langle \delta P^2 \rangle)/(2k_B T)]}{\omega_{vm}^{\text{PTO}}(q, a_1, a_{11}, P_r^2, \langle \delta P^2 \rangle)} \frac{d\mathbf{q}}{(2\pi)^3}, \quad (\text{S25})$$

where the energy spectrum $\hbar\omega_{vm}^{\text{PTO}}(q, a_1, a_{11}, P_r^2, \langle \delta P^2 \rangle) = \hbar\sqrt{\Delta_{\text{PTO}}^2(a_1, a_{11}, P_r^2, \langle \delta P^2 \rangle) + gq^2/m_p}$ with the excitation gap:

$$\begin{aligned} \Delta_{\text{PTO}}(a_1, a_{11}, P_r^2, \langle \delta P^2 \rangle) = & \left\{ a_1 + \left(\frac{a_{11}}{3} + \frac{4a_{12}}{3}\right)P_r^2 + \left(\frac{a_{111}}{3} + \frac{4a_{112}}{3}\right)P_r^4 + \left[\frac{a_{11}}{3} + \frac{4a_{12}}{3} + \left(\frac{4a_{123}}{9} + \frac{2a_{111}}{9} + \frac{8a_{112}}{3}\right)P_r^2\right]\langle \delta P^2 \rangle \right. \\ & \left. + \left(\frac{a_{111}}{9} + \frac{4a_{112}}{3} + \frac{2a_{123}}{9}\right)\langle \delta P^2 \rangle^2 \right\}^{1/2} / \sqrt{m_p}. \end{aligned} \quad (\text{S26})$$

Consequently, following the self-consistent renormalization processes in the main text, one can use the ground-state parameters to produce the dielectric/ferroelectric properties of the ferroelectric PbTiO₃ at finite temperatures. For the accuracy, we directly start with the experimentally measured zero-temperature parameters and perform the renormalization by the thermal fluctuations:

$$\alpha = a_1^{(0)} + \left(\frac{a_{11}^{(0)}}{3} + \frac{4a_{12}}{3}\right)\langle \delta P_{\text{th}}^2 \rangle + \left(\frac{a_{111}}{9} + \frac{4a_{112}}{3} + \frac{2a_{123}}{9}\right)\langle \delta P_{\text{th}}^2 \rangle^2 + \delta\alpha(T), \quad (\text{S27})$$

$$\beta = a_{11}^{(0)} + \left(\frac{2a_{111}}{3} + \frac{8a_{112}}{3}\right)\langle \delta P_{\text{th}}^2 \rangle, \quad (\text{S28})$$

$$\lambda = a_{111}, \quad (\text{S29})$$

$$\langle \delta P_{\text{th}}^2 \rangle = \int \frac{\hbar}{2m_p} \left\{ \frac{\coth[\hbar\omega_{vm}^{\text{PTO}}(q, a_1^{(0)}, a_{11}^{(0)}, P_r^2, \langle \delta P_{\text{th}}^2 \rangle)/(2k_B T)]}{\omega_{vm}^{\text{PTO}}(q, a_1^{(0)}, a_{11}^{(0)}, P_r^2, \langle \delta P_{\text{th}}^2 \rangle)} - \frac{1}{\omega_{vm}^{\text{PTO}}(q, a_1^{(0)}, a_{11}^{(0)}, P_r^2, 0)} \right\} \frac{d\mathbf{q}}{(2\pi)^3}, \quad (\text{S30})$$

where $a_1^{(0)}$ and $a_{11}^{(0)}$ are the zero-temperature parameters, and here we have introduced a correction/perturbation term $\delta\alpha(T)$. The correction due to the coupling of the polarization field with the gapless acoustic phonons through the electrostrictive effect should manifest with characteristic features at low temperatures, but in the ferroelectric phase is masked by the large $1/\varepsilon$ at low T . The

correction by this coupling is therefore minimal and can be neglected in the ferroelectrics. However, in the ferroelectric phase, the increased polarization fluctuation with temperature can cause the lattice vibrations and structural instabilities, which influence the harmonic potentials of all lattice degrees of freedom in the self-consistent phonon-field approximation [14], and hence, the imaginary frequencies of the unstable phonon mode. To characterize this effect, we follow the treatment of the fluctuations for the pinning and depinning behaviors in the charge-density waves by using the self-consistent field approximation [15, 16], and the corresponding correction in the ferroelectrics is written as [15, 16]

$$\delta\alpha(T) = -\eta a_0 \exp\left[-P_r^2/\langle\delta P_{\text{th}}^2(T)\rangle\right], \quad (\text{S31})$$

with $\eta < 1$ being a small dimensionless coefficient. It should be emphasized that $\delta\alpha(T)$ vanishes at $T = 0$ and contributes to a small correction $-\eta a_0$ near the phase transition point.

TABLE SI: Specific model parameters used in our thermodynamic theory for the classical ferroelectric PbTiO₃. The temperature-independent a_{12} , a_{111} , a_{112} and a_{123} are from Ref. [11] according to the experimental data at room temperature, whereas the zero-temperature parameters $a_1^{(0)}$ and $a_{11}^{(0)}$ are determined in order to give the experimental estimate $P_r \sim 63 \mu\text{C}/\text{cm}^2$ [17] and $\varepsilon = 167$ [18] for the zero temperature. Δ_{op} and v_{op} of the observed optical soft-phonon mode of the ferroelectric state are extracted from the experimental data of the inelastic neutron scattering measurement [19]. The wave-vector cutoff $q_{\text{c,FE}}$ in the integral of the bosonic excitation of the collective vector mode is taken as the Debye wave-vector cutoff. The parameter related to the correction term is set as $\eta = 0.1$.

$a_1^{(0)}$ ($\text{\AA}\cdot\text{meV}$)	$-0.1 \times 10^4/6.24$	$a_{11}^{(0)}$ ($\text{\AA}^5\cdot\text{meV}/\text{e}^4$)	$-3.6 \times 10^7/(6.24)^3$	a_{12} ($\text{\AA}^5\cdot\text{meV}/\text{e}^4$)	$7.5 \times 10^7/(6.24)^3$
a_{111} ($\text{\AA}^9\cdot\text{meV}/\text{e}^6$)	$1.6 \times 10^{12}/(6.24)^5$	a_{123} ($\text{\AA}^9\cdot\text{meV}/\text{e}^6$)	$-3.66 \times 10^{12}/(6.24)^5$	a_{112} ($\text{\AA}^9\cdot\text{meV}/\text{e}^6$)	$6.1 \times 10^{11}/(6.24)^5$
v_{op} ($\text{\AA}/\text{ps}$)	52.1	$q_{\text{c,FE}}$	$q_D = (6N\pi^2/\Omega_{\text{cell}})^{1/3}$	$\hbar\Delta_{\text{op}}$ (meV)	11

Classical criticality of an ordered ferroelectric phase

We discuss the criticality of an ordered ferroelectric phase in this section. For a simplified analysis, we use the model in the main text and consider the corresponding zero-temperature parameters $a_0 < 0$, $b_0 \neq 0$ and $\lambda \neq 0$.

Due to the gapped collective vector mode, below the temperature $\hbar\Delta_{\text{op}}/k_B \approx 127$ K, the thermal fluctuation of the polarization is minimal, leading to the dielectric properties insensitive to the temperature variation. When the increase in temperature exceeds above $\hbar\omega_{\text{vm}}(q_c)/k_B$, with q_c being the wave-vector cutoff, the excitation gap Δ persists, and by Eq. (16) in the main text, one finds approximately

$$\langle\delta P_{\text{th}}^2\rangle \approx k_B T \int_0^{q_c} \frac{\hbar q^2 dq / (2\pi)^2}{m_p \Delta^2 + g q^2} = k_B T \left[\sqrt{g q_c^2} - \sqrt{m_p \Delta^2} \arctan\left(\sqrt{g q_c^2 / (m_p \Delta^2)}\right) \right] \frac{\hbar}{g^{3/2} (2\pi)^2}. \quad (\text{S32})$$

For $g q_c^2 / (m_p \Delta^2) \gg 1$ as usually observed in the ferroelectric materials, $\langle\delta P_{\text{th}}^2\rangle$ exhibits the linear- T behavior, leading to the widely reported classical linear- T dependencies in $1/\varepsilon(T)$ and $\alpha(T)$ in the literature.

However, with further increase in temperature, the increased $\delta P_{\text{th}}^2(T)$ approaches the reduced $P_r^2(T)$, i.e., $\delta P_{\text{th}}^2(T) \sim P_r^2(T)$. In this regime, the excitation gap in Eq. (6) in the main text becomes

$$\begin{aligned} m_p \Delta^2 &= a_0 + b_0(2/d_p + 1)\langle\delta P_{\text{th}}^2\rangle + \lambda(4/d_p + 1)\langle\delta P_{\text{th}}^2\rangle^2 + [b_0 + 2\lambda(4/d_p + 1)\langle\delta P_{\text{th}}^2\rangle]\langle\delta P_{\text{th}}^2\rangle + \lambda\langle\delta P_{\text{th}}^2\rangle^2 \\ &= \alpha + \beta\langle\delta P_{\text{th}}^2\rangle + \lambda\langle\delta P_{\text{th}}^2\rangle^2 = \alpha + \beta P_r^2 + \lambda P_r^4 = 0. \end{aligned} \quad (\text{S33})$$

Here, we have used the expressions for the free-energy parameters α and β [Eqs. (14) and (15) in the main text] as well as P_r^2 . Consequently, when the thermal fluctuation $\delta P_{\text{th}}^2(T)$ approaches the order parameter P_r^2 , the excitation gap of the collective vector mode nearly vanishes, and this in turn leads to a rapidly enhanced fluctuation and hence $\alpha(T)$ towards zero (i.e., breaking of the phase), leading to the phase transition.

TABLE III: Specific parameters used in our thermodynamic theory for the quantum paraelectric SrTiO₃. For the model parameters at zero temperature, v_{op} and Δ_{op} of the optical soft-phonon mode of the incipient ferroelectric state are from Ref. [10] by comparing the data from inelastic neutron [20] and Raman scattering [21] experiments at 4 K, and a_0 and b_0 are from Ref. [10] by measuring $E/P = a_0 + b_0 P^2$ at 0.3 K, with E being the electric field (0 to 15 kV/cm) and P denoting the electric polarization. The wave-vector cutoff $q_{\text{c,FE}}$ in the integral for the bosonic excitation of the collective vector mode, which determines the Curie–Weiss behavior as shown by Eq. (S19), is extracted from the Curie constant in the experimental data [10]. As for the correction from the acoustic phonons, the group velocity of the acoustic phonon modes, v_{LA} (longitudinal acoustic mode) and $v_{\text{TA,(1)}}$ (transverse acoustic mode) are given in Ref. [22] by experimental measurement. Moreover, Ref. [23] reported the disappearance of a transverse acoustic phonon branch in SrTiO₃ at low temperatures, due to the coupling with the optical phonon of the incipient ferroelectric instability near the quantum critical point, and this mode is sometimes referred to as the second sound in the literature. Here we take account of this anomalous disappearance by, as an approximation, considering a softening of this acoustic phonon branch, i.e., an effectively reduced group velocity $v_{\text{TA,(2)}}$, which is determined by taking the recently reported/estimated group velocity from the thermal-conductivity measurement near the tetragonal phase of SrTiO₃ [24]. The cubic electrostrictive constant C is determined by the first-principles method and it shows good agreement with the experimental data of strain [25]. The wave-vector cutoff $q_{\text{c,AC}}$ in the integral of the acoustic phonons is chosen to fit the minimum (single point) of the dielectric function at the low-temperature limit. We noticed that there could be a hot effect during the measurement in Ref. [10], and in consideration of this effect, the experimental data of SrTiO₃ in Fig. 2 in the main text have been shifted by 1.66 K toward the high-temperature direction.

model parameters		acoustic-phonon correction	
a_0 (meV·Å/e ²)	$5.061 \times 10^{-5} / \epsilon_0$	v_{LA} (Å/ps)	78.66
b_0 (meV·Å ⁵ /e ⁴)	$0.07 \times (2\pi)^3 / \epsilon_0$	$v_{\text{TA,(1)}}$ (Å/ps)	49.04
$\hbar\Delta_{\text{op}}/k_B$ (K)	24	$v_{\text{TA,(2)}}$ (Å/ps)	10
v_{op} (Å/ps)	81	d_{111} (meV/Å ³)	$-5 \times 10^4 / 1.6$
$q_{\text{c,FE}}$ (Å ⁻¹)	0.67	$3d_{144}$ (meV/Å ³)	$-2 \times 10^4 / 1.6$
		C (meV·Å/e ²)	24.08 a_0
		$q_{\text{c,AC}}$ (Å ⁻¹)	0.15

Parameters used in the numerical simulation based on our thermodynamic theory for the renormalization by thermal fluctuations

In this part, we present the specific values of the used zero-temperature parameters in the simulation and the way in which they were determined. According to the lattice dynamics of the unstable phonon mode, the polarization inertia is given by [13, 37]

$$m_p = \frac{\Omega_{\text{cell}}}{\sum_i Q_i^2 / M_i}, \quad (\text{S34})$$

where M_i and Q_i denote the ionic masses and charges in the unit cell of volume Ω_{cell} , respectively. Moreover, because of the lattice dynamics, the coefficient g is related to the velocity v_{op} of the imaginary-frequency phonons ($\omega_{\text{im}}^2 = -\Delta_{\text{im}}^2 + v_{\text{op}}^2 q^2$) of the ferroelectrics and is written as

$$g/m_p = \nu v_{\text{op}}^2, \quad (\text{S35})$$

where $\nu = \Omega_{\text{im}} / \Omega_{\text{total}}^{\text{eff}} < 1$ is the condensation ratio (with Ω_{im} being the volume of the momentum space of the imaginary-frequency phonons and $\Omega_{\text{total}}^{\text{eff}}$ denoting an effective total volume) and is taken as $\nu = \Delta^2(a_0, b_0, P_0^2, 0) / \Delta_{\text{op}}^2$ following the treatment in Ref. [10] as a consequence of the condensation. Here, Δ_{op} denotes the excitation gap of the experimentally observed optical soft phonon mode ($\omega_{\text{op}}^2 = \Delta_{\text{op}}^2 + v_{\text{op}}^2 q^2$) of the ferroelectric state at low-temperature limit. Other used specific parameters in the developed thermodynamic theory for the classical ferroelectric PbTiO₃ as well as quantum paraelectric SrTiO₃ and KTaO₃ are addressed in Tables SI as well as SII and SIII, respectively.

Renormalization by zero-point fluctuations

We show in this part that the renormalization by the zero-point fluctuations on the bare parameters is important for accurate predictions as compared with the experimental measurements at low-temperature limit. In principle, the formulation of the bare parameters in the displacive ferroelectrics is usually associated with the structural/lattice instabilities. It therefore requires the first-principles calculation with highly accurate computation of the self-consistent harmonic lattice dynamics and higher-level treatment of the electronic correlation. Since similar formulation has recently been performed in SrTiO₃ [14], we take SrTiO₃ as the example here.

TABLE III: Specific parameters used in our thermodynamic theory for the quantum paraelectric KTaO_3 . For the model parameters at zero temperature, $v_{\text{op}} = 57 \text{ \AA/ps}$ and $\hbar\Delta_{\text{op}}/k_B = 36 \text{ K}$ of the optical soft-phonon mode of the incipient ferroelectric state were determined in Ref. [10] by comparing the data from inelastic neutron [26] and Raman scattering [21] experiments at 4 K. In the simulation for each experiment, a_0 is extracted from the measured $1/\varepsilon(T)$ near $T = 0$, and b_0 is determined by $1/\varepsilon(T = 10 \text{ K})$. The wave-vector cutoff $q_{\text{c,FE}}$ in the integral for the bosonic excitation of the collective vector mode, which determines the Curie–Weiss behavior as shown by Eq. (S19), is extracted from the Curie constant in each experiment. As for the correction from the acoustic phonons, the group velocity of the acoustic phonon modes, v_{LA} and $v_{\text{TA,(1)}}$, are given in Ref. [27] through various approaches, and the second-sound velocity $v_{\text{TA,(2)}}$ comes from Refs. [28–30]. The cubic electrostrictive constant C is determined by the experimental finding that the strain-induced ferroelectric phase transition occurs at a critical stress $\sigma_c = 5.5 \times 10^9 \text{ dyn/cm}^2$ [31], i.e., $C = (1/s_c)a_0$ with the critical strain s_c determined by the critical equation $2c_{11}s_c + 3d_{111}s_c^2 + \sigma_c = 0$. The strain coefficients c_{11} , d_{111} and d_{144} were addressed in Ref. [32]. The wave-vector cutoff $q_{\text{c,AC}}$ in the integral of the acoustic phonons is chosen to fit the minimum (single point) of the dielectric function at low-temperature limit in Ref. [10]. We noticed that there could be a hot effect during the measurement in Ref. [10], and in consideration of this effect, the experimental data of KTaO_3 in Fig. 3 in the main text have been shifted by 2.5 K toward the high-temperature direction.

model parameters	a_0 (meV·Å/e ²)	b_0 (meV·Å ⁵ /e ⁴)	$q_{\text{c,FE}}$ (Å ⁻¹)	
for EXP in Ref. [10]	$22 \times 10^{-5}/\varepsilon_0$	$0.2 \times (2\pi)^3/\varepsilon_0$	0.65	
for EXP in Ref. [33]	$22.7 \times 10^{-5}/\varepsilon_0$	$0.3 \times (2\pi)^3/\varepsilon_0$	0.486	
for EXP in Ref. [34]	$25 \times 10^{-5}/\varepsilon_0$	$0.3 \times (2\pi)^3/\varepsilon_0$	0.469	
for EXP in Ref. [35]	$23 \times 10^{-5}/\varepsilon_0$	$0.29 \times (2\pi)^3/\varepsilon_0$	0.553	
for EXP in Ref. [36]	$20.1 \times 10^{-5}/\varepsilon_0$	$0.16 \times (2\pi)^3/\varepsilon_0$	0.52	
acoustic-phonon correction	v_{LA}	$v_{\text{TA,(1)}}$	$v_{\text{TA,(2)}}$	C (meV·Å/e ²)
	75	44	10	$22a_0$
	d_{111} (meV/Å ³)	$3d_{144}$ (meV/Å ³)	$q_{\text{c,AC}}$ (Å ⁻¹)	c_{11} (meV/Å ³)
	$-5.5 \times 10^4/1.6$	$-1.2 \times 10^4/1.6$	0.23	0.37/1.6

The first-principles calculation adopting the PBEsol/rSCAN functional in Ref. [14] reported the unstable phonon modes with imaginary frequencies (i.e., negative values of the harmonic terms in lattice dynamics) at the Γ point in cubic phase of SrTiO_3 . According to the lattice dynamics and condensation of the imaginary-frequency phonons ($\omega_{\text{im}}^2 = -\Delta_{\text{im}}^2 + v_{\text{op}}^2 q^2$), one has $a = -\nu m_p \Delta_{\text{im}}^2$, with $\nu < 1$ being the condensation ratio, and hence, the imaginary frequencies result in a negative value of the bare parameter a . For SrTiO_3 , with the calculated $\hbar\Delta_{\text{im}} \approx 7.7 \text{ meV}$ from PBEsol functional [14], one has $a = -70.15 \times 10^{-5}/\varepsilon_0$, suggesting a ferroelectric ground state of SrTiO_3 at the bare case. Then, from the self-consistent renormalization by the zero-point fluctuations in the developed thermodynamic theory [Eqs. (11)-(13) in the main text], taking the wave-vector cutoff in the integral of the zero-point oscillations of the collective vector mode as the Debye wave-vector cutoff $q_D = (6N\pi^2/\Omega_{\text{cell}})^{1/3}$ for the quantum fluctuations, our numerical calculation predicts $a_{0,\text{zo}} \approx 3.25 \times 10^{-5}/\varepsilon_0$, in good agreement with the experimentally measured one $a_0 \approx 5.06 \times 10^{-5}/\varepsilon_0$ (Table SII). In other words, because of the existence of the unstable phonon mode, SrTiO_3 should undergo a transition to the ferroelectric phase at low temperatures, but the zero-point oscillation/vibration of the collective vector mode prevents the formation of the long-range ferroelectric ordering, leading to an incipient ferroelectricity (quantum paraelectric state). This theoretical/analytical description confirms the established understanding of the quantum paraelectric ground state of SrTiO_3 in the literature, while Ref. [14] has also reported that when the self-consistent quantum anharmonic fluctuations are accounted for in the first-principles calculation, the original unstable phonon modes at the Γ point are found to be stable. Consequently, in the quantum paraelectrics, the bare state is ferroelectric but the zero-temperature state is paraelectric. Because of this unique character, the collective vector mode can persist to exist and be uninterrupted in a wide temperature range above zero temperature. This also leads to an interesting open question in the further investigation that whether the ground state of the quantum paraelectrics can be interpreted as a state that contains the creation and annihilation of the many-particle condensation, similar to the quantum-field vacuum state that contains the creation and annihilation of the various single particles.

* Electronic address: fzy5099@psu.edu

† Electronic address: lqc3@psu.edu

[1] F. Yang and L.-Q. Chen, arXiv:2410.05216 (2024).

[2] F. Yang and M. Wu, Phys. Rev. B **104**, 214510 (2021).

[3] F. Yang and M. Wu, Phys. Rev. B **106**, 144509 (2022).

- [4] Z. Sun, M. Fogler, D. Basov, and A. J. Millis, *Phys. Rev. Res.* **2**, 023413 (2020).
- [5] A. A. Abrikosov, L. P. Gorkov, and I. E. Dzyaloshinski, *Methods of quantum field theory in statistical physics* (Prentice Hall, Englewood Cliffs, 1963).
- [6] M. E. Peskin, *An introduction to quantum field theory* (CRC press, 2018).
- [7] F. Yang and M. Wu, *Phys. Rev. B* **102**, 014511 (2020).
- [8] L. Palova, P. Chandra, and P. Coleman, *Phys. Rev. B* **79**, 075101 (2009).
- [9] D. Khmel'nitskii and V. Shneerson, *Zh. Eksp. Teor. Fiz* **64**, 316 (1973).
- [10] S. Rowley, L. Spalek, R. Smith, M. Dean, M. Itoh, J. Scott, G. Lonzarich, and S. Saxena, *Nat. Phys.* **10**, 367 (2014).
- [11] M. J. Haun, E. Furman, S. Jang, H. McKinstry, and L. Cross, *J. Appl. Phys.* **62**, 3331 (1987).
- [12] L. Landau, E. Lifshitz, and L. E. Reichl, *Statistical physics, part 1* (American Institute of Physics, 1981).
- [13] P. Tang, R. Iguchi, K.-i. Uchida, and G. E. Bauer, *Phys. Rev. B* **106**, L081105 (2022).
- [14] C. Verdi, L. Ranalli, C. Franchini, and G. Kresse, *Phys. Rev. Mater.* **7**, L030801 (2023).
- [15] K. Maki, *Phys. Rev. B* **33**, 2852 (1986).
- [16] T. Rice, S. Whitehouse, and P. Littlewood, *Phys. Rev. B* **24**, 2751 (1981).
- [17] J. Remeika and A. Glass, *Mater. Res. Bull.* **5**, 37 (1970).
- [18] S. Ikegami, I. Ueda, and T. Nagata, *J. Acoust. Soc. Am.* **50**, 1060 (1971).
- [19] J. Hlinka, M. Kempa, J. Kulda, P. Bourges, A. Kania, and J. Petzelt, *Phys. Rev. B* **73**, 140101 (2006).
- [20] Y. Yamada and G. Shirane, *J. Phys. Soc. Jpn.* **26**, 396 (1969).
- [21] P. Fleury and J. Worlock, *Phys. Rev.* **174**, 613 (1968).
- [22] S. Kor and N. Tripathi, *J. Phys. Soc. Jpn.* **38**, 1073 (1975).
- [23] X. He, D. Bansal, B. Winn, S. Chi, L. Boatner, and O. Delaire, *Phys. Rev. Lett.* **124**, 145901 (2020).
- [24] Z. Zhang, K. Yuan, J. Zhu, X. Fan, J. Zhou, and D. Tang, *Appl. Phys. Lett.* **120** (2022).
- [25] T. Shimizu, *Solid State Commun.* **102**, 523 (1997).
- [26] G. Shirane, R. Nathans, and V. Minkiewicz, *Phys. Rev.* **157**, 396 (1967).
- [27] Y.-Q. Xu, S.-Y. Wu, L.-J. Zhang, L.-N. Wu, and C.-C. Ding, *Phys. Status Solid* **254**, 1600620 (2017).
- [28] A. Koreeda, R. Takano, A. Ushio, and S. Saikan, *Phys. Rev. B* **82**, 125103 (2010).
- [29] E. Farhi, A. Tagantsev, B. Hehlen, R. Currat, L. Boatner, and E. Courtens, *Ferroelectrics* **239**, 25 (2000).
- [30] E. Farhi, A. Tagantsev, B. Hehlen, R. Currat, L. Boatner, and E. Courtens, *Physica B Condens. Matter* **276**, 274 (2000).
- [31] H. Uwe and T. Sakudo, *J. Phys. Soc. Jpn.* **38**, 183 (1975).
- [32] B. Achar, G. Barsch, and L. Cross, *Ferroelectrics* **37**, 495 (1981).
- [33] S. Wemple, *Phys. Rev.* **137**, A1575 (1965).
- [34] W. Abel, *Phys. Rev. B* **4**, 2696 (1971).
- [35] C. Ang, A. Bhalla, and L. Cross, *Phys. Rev. B* **64**, 184104 (2001).
- [36] O. Aktas, S. Crossley, M. A. Carpenter, and E. K. Salje, *Phys. Rev. B* **90**, 165309 (2014).
- [37] S. Sivasubramanian, A. Widom, and Y. Srivastava, *Ferroelectrics* **300**, 43 (2004).